Coordination Chemistry Reviews 548 (2026) 217163

Contents lists available at ScienceDirect

Coordination Chemistry Reviews

journal homepage: www.elsevier.com/locate/ccr

Cascade nanozymes as ROS scavengers for the treatment of aseptic inflammation

Qing Miao [a,b], Hongyu Yang [a,b], Xinyuan Zhu [a], Xuesong Feng [b,*], Jinghui Yang [c,*], Youfu Wang [a,*]

[a] School of Chemistry and Chemical Engineering, Frontiers Science Center for Transformative Molecules, Shanghai Jiao Tong University, Shanghai 200240, China.
[b] School of Pharmacy, China Medical University, Shenyang 110122, China.
[c] Department of Organ Transplantation, Shanghai Changzheng Hospital, Naval Medical University, Shanghai 200003, China.

ARTICLE INFO

Keywords:
Nanozymes
Cascade catalysis
Aseptic inflammation
Reactive oxygen species
Antioxidation

ABSTRACT

Aseptic inflammatory diseases, including autoimmune disorders and chronic tissue injuries, pose significant health challenges globally, with ROS playing a key pathogenic role. While nanozymes have been explored as ROS scavengers for anti-inflammatory therapy, their clinical application is limited by suboptimal catalytic performance. Recent advances focus on cascade nanozymes, which integrate multiple enzymatic activities to mimic natural metabolic pathways. These cascade nanozymes are classified into linear, triangular, cyclic, orthogonal, and parallel configurations, each offering distinct advantages in spatial organization and sequential reaction control. Cascade nanozymes combine the stability and reusability of traditional nanozymes with enhanced catalytic efficiency, reducing diffusion barriers and improving intermediate utilization. By precisely modulating inflammatory responses, they mitigate oxidative stress and cytokine overproduction while preserving host defense mechanisms. This review highlights technological progress, applications, challenges, and future directions in cascade nanozyme development, paving the way for improved functional validation and therapeutic innovation.

1. Introduction

Inflammation [1–3] is a protective and adaptive physiological response elicited by biological organisms to counteract tissue damage, pathogen invasion, or exposure to harmful stimuli. It can be broadly categorized into two types: aseptic inflammation and pathogen-associated inflammation [4–6]. Although two share overlapping clinical manifestations but differ fundamentally in their underlying pathogenic mechanisms. In terms of pathogenic mechanisms, pathogen-associated inflammatory diseases are primarily driven by the invasion of exogenous pathogens such as bacteria, viruses, or fungi. These pathogens express pathogen-associated molecular patterns (PAMPs) [7–9], including lipopolysaccharides (LPS), flagellin, or viral nucleic acids, which are recognized by the host's innate immune system through pattern recognition receptors (PRRs) [10] such as Toll-like receptors (TLRs) [11,12], NOD-like receptors (NLRs) [13,14], and RIG-I-like receptors (RLRs) [15]. This recognition initiates a cascade of intracellular signaling pathways, leading to the activation of transcription factors like Nuclear factor kappa B (NF-κB) [16–18] and the subsequent production of pro-inflammatory cytokines such as TNF-α, IL-6, and IL-12. These cytokines orchestrate a coordinated immune response aimed at eliminating the invading pathogen and initiating tissue repair. In contrast, aseptic inflammation [19–21] arises in the absence of microbial infection and is typically triggered by endogenous damage-associated molecular patterns (DAMPs) [22,23]. DAMPs, such as high-mobility group box 1 (HMGB1), heat shock proteins, ATP, and uric acid crystals, are released from necrotic or stressed cells following tissue injury, ischemia, or autoimmune processes. These molecules also engage PRRs, particularly the NLRP3 inflammasome [24–28], leading to the activation of caspase-1 and the subsequent cleavage and release of mature IL-1β and IL-18. Unlike pathogen-induced inflammation, which is usually self-limiting and resolves after pathogen clearance, aseptic inflammation can persist indefinitely, contributing to various acute/chronic diseases.

Although its complete mechanisms remain to be fully elucidated, the aseptic inflammatory is primarily initiated by endogenous danger signals, particularly reactive oxygen species (ROS) [29–31] generated

* Corresponding authors.
E-mail addresses: xsfeng@cmu.edu.cn (X. Feng), yjh@smmu.edu.cn (J. Yang), wyfown@sjtu.edu.cn (Y. Wang).

https://doi.org/10.1016/j.ccr.2025.217163
Received 18 July 2025; Accepted 4 September 2025
Available online 11 September 2025

during cellular stress [32], mechanical injury, or chemical exposure. The initial phase features ROS-mediated oxidation of sensor proteins that potentiate pattern recognition receptor activation, thereby enhancing their capacity to detect DAMPs. Subsequent nicotinamide adenine dinucleotide Phosphate (NADPH) oxidase-dependent [33,34] ROS generation amplifies cytokine cascades and leukocyte infiltration while concurrently regulating redox-sensitive transcription factors, establishing a self-sustaining inflammatory milieu. Experimental evidence confirms the essential signaling role of ROS in orchestrating inflammatory responses through modulation of multiple pathways, including the NLRP3 (NOD-, LRR- and pyrin domain-containing protein 3) inflammasome assembly, NF-κB activation cascade, and MAPK (mitogen-activated protein kinase) signaling network [35,36]. The dual functionality of ROS arises from their high chemical reactivity-while functioning as pivotal signaling molecules, they simultaneously induce cellular damage through oxidation of critical biomolecules including proteins, lipids, and nucleic acids. Thus, maintaining ROS homeostasis at basal levels emerges as a critical regulatory mechanism for preventing pathological exacerbation of aseptic inflammation.

The endogenous antioxidant system [37–39] represents an essential biological mechanism for counteracting oxidative stress under physiological conditions. The ROS homeostasis is maintained through sophisticated antioxidant networks, with enzymatic antioxidants constituting the principal defense system. Some core enzymes like superoxide dismutase (SOD) [40–42], catalase (CAT) [43,44], glucose oxidase (GOx) [45,46], NADPH oxidase (NOX) [47–49], peroxidase (POD) [50,51], and glutathione peroxidase (GPx) [52] demonstrate ubiquitous tissue distribution and perform vital functions in scavenging reactive intermediates and preserving cellular redox balance. These enzymes operate through sequential biochemical transformations: SOD catalyzes $\cdot O_2^-$ dismutation to H_2O_2, subsequently processed by CAT and GPx into water and oxygen, while POD facilitates complementary redox cycles via electron donor systems. GPx-like activity plays a crucial role in the cellular defense system, particularly in the elimination of H_2O_2. This process involves the catalytic conversion of GSH, the major intracellular antioxidant, into its oxidized form, GSSG, as part of the redox reaction that neutralizes harmful peroxides. In a healthy cell, the regeneration of GSH occurs through the action of NADPH-dependent glutathione reductase (GR), an enzyme that catalyzes the reduction of GSSG back to GSH. Thus, the GPx-like activity of nanozymes, which involves the consumption of GSH, contributes to the mitigation of oxidative damage and the maintenance of cellular redox homeostasis. This preserved cellular homeostasis, in turn, ensures a continuous supply of reduced GSH within an undamaged cell. GOx activity is characterized by the highly specific, oxygen-dependent oxidation of glucose to gluconic acid, concomitantly generating H_2O_2. NOX activity mitigates inflammatory damage through its catalytic function in producing bioactive nitric oxide (NO) at physiologically relevant flux levels. Nevertheless, native antioxidant enzymes exhibit intrinsic limitations that constrain therapeutic applications. Critical challenges include restricted operational stability under physiological pH and temperature conditions, susceptibility to proteolytic degradation, and transient circulatory persistence. Consequently, there is an urgent need to develop antioxidant systems that integrate the catalytic activity of natural enzymes with structural robustness. Nanozymes, which combine the physicochemical and biological properties of nanomaterials with enzyme-like catalytic functions, have garnered significant attention due to their structural stability, multifunctionality, cost-effectiveness, reusability, and scalability in production and storage. Leveraging these properties, various nanozymes have been designed and applied in the treatment of aseptic inflammatory diseases [53,54] demonstrating promising prospects and potential. However, conventional nanozymes face inherent limitations in treatment performance due to their monotonous biocatalytic activity. This fundamental limitation has prompted the development of cascade nanozymes that mimic natural enzyme cooperation.

A cascade refers to a sequential chain reaction triggered by precursor events, where upstream products or signals activate downstream steps, leading to exponential amplification of reaction efficiency and signal intensity. Compared to conventional biomedical nanozymes, these biomimetic systems exhibit three distinguishing characteristics in biomedical applications [55,56]: (i) High atom economy with reduced reaction steps and enhanced process efficiency; (ii) Spatially confined reaction sites that minimize diffusion distances and increase local concentrations of intermediates; (iii) Accelerated mass transfer coupled with minimized intermediate decomposition, synergistically boosting overall cascade reaction efficiency.

Building upon the demonstrated success of cascade nanozymes in aseptic inflammation, this review systematically elucidates the therapeutic mechanisms and translational progress of such nanoscale catalytic platforms in addressing critical inflammatory pathologies, including inflammatory bowel disease, osteoarthritis, rheumatoid arthritis, diabetic complications, liver disease, acute kidney injury, cardiovascular disorders, ischemic stroke, neuroinflammation, and spinal cord injury (Fig. 1).

2. Nanozyme-based cascade catalysis systems

Nanozyme-based cascade systems [57,58] embody innovative biomimetic architectures that replicate natural enzymatic cooperation through coordinated catalytic sequences. These systems demonstrate progressively amplified therapeutic effects via staged molecular transformations, where initial reaction products become substrates for subsequent enzymatic actions. The sources of these cascading activities [59–63] mainly come from the valence state changes of metal species, the inherent structures (such as surface defects), and dispersed states of metals (single atom or aggregation). Current classification frameworks identify five distinct cascade configurations [64–66] based on their kinetic coordination patterns and spatial organization principles (Fig. 2).

Linear cascades [67] operate through unidirectional substrate conversion pathways, particularly effective in acute oxidative environments. SOD-CAT configurations exemplify this approach, where sequential dismutation of $\cdot O_2^-$ by SOD and subsequent H_2O_2 decomposition by CAT achieves comprehensive free radical neutralization. Li et al. [68] constructed a SOD-CAT cascade catalytic system by

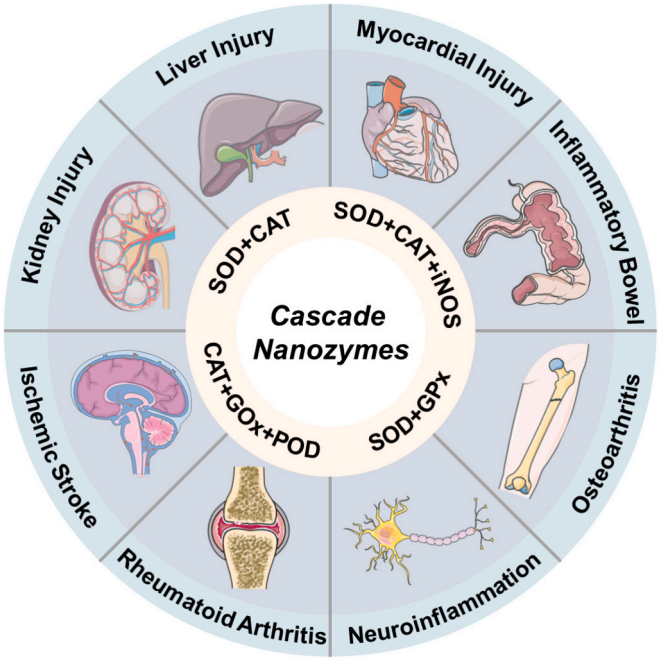

Fig. 1. Applications of cascade nanozymes for the treatment of various aseptic inflammation.

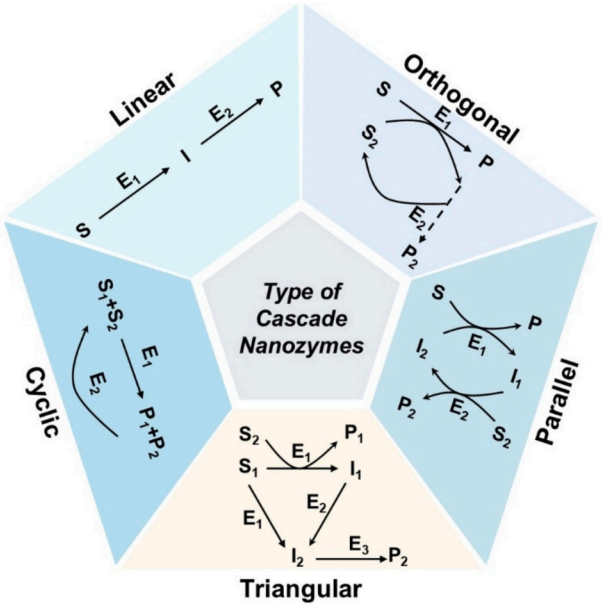

Fig. 2. Types of cascaded nanozymes. $S_{1/2}$: substrate; $E_{1/2/3}$: enzyme; $I_{1/2}$: intermediate product; P/P_2: desired product; P_1: by-product.

integrating Pd nanoclusters with CoPcS-$Ti_3C_2T_x$ nanocomposites through non-covalent π-π conjugation. This hybrid nanozyme, composed of sulfonated cobalt phthalocyanine (CoPcS) and titanium carbide ($Ti_3C_2T_x$) nanosheets, demonstrates robust SOD-CAT mimetic activity for the treatment of osteoarthritis. The enhanced enzymatic performance arises from efficient electron transfer at the Pd/CoPcS-$Ti_3C_2T_x$ interface, which concurrently enhances radical adsorption energy and reduces the energy barrier of the SOD-CAT cascade reaction, thereby accelerating the overall reaction kinetics. Compared to single-enzyme systems, cascade catalysis offers superior safety by converting unstable or toxic intermediates promptly with minimal side reactions. Its linear architecture features strictly sequential and irreversible reaction chains, requiring optimization of kinetic bottlenecks to maximize catalytic efficiency.

Cyclic cascades [69] establish self-renewing catalytic loops, maintaining sustained antioxidant activity crucial for chronic inflammatory conditions. The GOx-CAT system illustrates this paradigm. Firstly, glucose is degraded into H_2O_2, which is further decomposed into H_2O and O_2 to complete the cascade reaction. Zhou et al. [70] developed a dual-nanozyme system comprising gold nanoparticles (Au NPs) with GOx-mimicking activity and iridium nanoparticles (Ir NPs) exhibiting CAT-like activity for diabetic retinopathy (DR) therapy. This system establishes a cascade mechanism that simultaneously alleviates hypoxia through continuous oxygen generation and scavenges microenvironmental peroxides, consequently reducing hyperglycemia and ameliorating oxidative stress. The distinguishing feature is that there is a reversible feedback path, and the advantage is that both the cofactor and the substrate can be fully recycled.

Orthogonal cascades [71] designs enable simultaneous non-interfering reactions through spatially segregated catalytic channels. This type of approach mainly involves multiple independent reactions occurring but not interfering with each other. Integrated SOD-CAT-POD-GPx exemplify this strategy, achieving multiplexed oxidative stress management. Liu et al. [72] engineered nitrogen-doped carbon encapsulated nanoceria (NCNC) nanozymes with integrated SOD-, CAT-, POD-, and GPx-mimetic activities for precision tumor therapy. Through strategic oxygen vacancy engineering, the NCNC system achieves an optimized Ce^{3+}/Ce^{4+} redox ratio that dynamically modulates enzymatic activities and activates dual catalytic pathways. The SOD-like activity first catalyzes $\cdot O_2^-$ disproportionation to generate H_2O_2, which subsequently fuels POD-like activity to produce cytotoxic ·OH. Simultaneously, CAT-like activity alleviates tumor hypoxia while GPx-like activity depletes glutathione, effectively improving the efficiency of tumor treatment.

Parallel cascades [73,74] optimize metabolic synergy through complementary enzymatic partnerships. Its feature concurrently operating, independent reaction chains interconnected through synergistic nodes, requiring multi-path coordination to achieve integrated outcomes. Tripartite systems combining POD, CAT, OXD, and NOX activities exemplify this approach, leveraging combined radical neutralization and peroxide reduction mechanisms. Zhou et al. [75] engineered a multifunctional platinum nanozyme composite (PFOB@PLGA@Pt) incorporating perfluorooctyl bromide (PFOB) for diabetic wound regeneration. The oxygen-releasing capacity of PFOB mitigates hypoxic conditions while potentiating Pt nanozyme's glucose oxidase-mimetic activity, driving glucose conversion to gluconic acid that establishes an acidic microenvironment. This pH shift sequentially activates NOX-, POD-, and OXD-mimetic activities to generate bactericidal ROS. Following bacterial eradication, endogenous SOD and CAT activities scavenge residual ROS, restoring redox equilibrium. Through autonomous pH-responsive switching of enzymatic functions, this nanoplatform achieves spatiotemporally regulated cascade catalysis for precision wound therapy.

Triangular cascades [76] implement redundant catalytic pathways to ensure reliability under fluctuating physiological conditions. In comparison to conventional systems, this approach exhibits enhanced therapeutic efficacy by enabling multi-targeted regulation of oxidative stress. Nevertheless, its widespread adoption remains constrained by the current complexity associated with implementation.

All cascade variants demonstrate dynamic responsiveness to cellular redox states, with emerging designs incorporating real-time activity modulation capabilities. Advanced systems employ multiple regulatory mechanisms including charge-dependent substrate interactions, temperature-responsive catalytic site accessibility, and oxidative stress-sensitive assembly processes. Below, we will discuss the synthesis strategies and biomedical applications of cascade nanozymes.

3. The application of Cascade Nanozymes in aseptic inflammation treatment

In recent years, the bio-application of cascade nanozymes has emerged as a prominent research focus. As a green chemical process, cascade reactions demonstrate high atom economy, minimal byproduct formation, and low energy consumption, thereby playing crucial roles in biological regulation, industrial catalysis, and most importantly, nanomedicine. This chapter summarizes the application of various cascade reactions in various aseptic inflammation diseases in recent years (Table 1).

3.1. *Inflammatory bowel disease*

Inflammatory bowel disease (IBD) [95–97] refers to a group of chronic inflammatory disorders affecting the gastrointestinal tract. The two primary types of IBD are ulcerative colitis (UC) and Crohn's disease (CD), both of which involve inflammation that may affect different parts of the digestive system. The exact cause of IBD remains unclear, but it is believed to involve an abnormal immune response against gut microbiota in genetically susceptible individuals. One of the key mechanisms underlying this abnormal immune response is the overproduction of ROS [98,99]. Excessive ROS levels not only exacerbate the inflammatory response by activating pro-inflammatory pathways, such as NF-κB and MAPKs, but also disrupt normal cellular functions. For instance, ROS can damage cellular components like lipids, proteins, and DNA, leading to impaired cell function and death. This oxidative damage further perpetuates the cycle of inflammation and tissue injury in IBD patients.

Recent advancements in nanozyme engineering have yielded

Table 1
Summary of biocatalytic cascade nanozymes in aseptic inflammation disease treatment.

Cascade nanozymes	Enzyme mimic	Reaction process	Kinetics	Ref
Au/CeO_2@HA	SOD, CAT	$O_2^{\cdot-} \xrightarrow{SOD} H_2O_2 \xrightarrow{CAT} O_2$	CAT: 6.33 U·mg^{-1}, K_m = 3.224 mM	[77]
Pd@M			CAT: K_m = 28.75 mM, V_{max} = 0.05 mg·L^{-1}·s^{-1}	[78]
KGN@HMZC@HA			–	[79]
Cu-TCPP-Mn			CAT: K_m = 34.65 mM, V_{max} = 0.01 mg·L^{-1}·s^{-1}	[80]
PNzyme/MnO_2			SOD: 2139.86 ± 234.90 U·mg^{-1} CAT: K_m = 4.9 ± 0.99 mM, V_{max} = (5.22 ± 0.23) × 10^{-2} M·s^{-1}	[81]
$^{IRF\text{-}5}$SiRNA@pMn	SOD, CAT, GPx	$O_2^{\cdot-} \xrightarrow{SOD} H_2O_2 \underset{GPx}{\overset{CAT}{\rightleftharpoons}} H_2O$	CAT: K_m = 48.13 mM, V_{max} = 17.09 M·s^{-1} GPx: K_m = 71.36 mM, V_{max} = 4.701 M·s^{-1}	[82]
DAGQD@Cu@KGN SAN	SOD, CAT, ·OH scavenging	$O_2^{\cdot-} \xrightarrow{SOD} H_2O_2 \xrightarrow{CAT} O_2$ $\cdot OH \xrightarrow[scavenging]{\cdot OH} H_2O$	–	[83]
PEI-Mn@curcumin	SOD, CAT, RNS scavenging	$O_2^{\cdot-} \xrightarrow{SOD} H_2O_2 \xrightarrow{CAT} O_2$ $RNS \xrightarrow[scavenging]{RNS} NO^{2-}/NO^{3-}/N_2O\ldots$	–	[84]
Mn_3O_4@CS	SOD, CAT, iNOS	$O_2^{\cdot-} \xrightarrow{SOD} H_2O_2 \xrightarrow{CAT} O_2 \xrightarrow{iNOS} NO$	SOD: K_m = 0.017 mM, V_{max} = 4.86 × 10^5 M·s^{-1} CAT: K_m = 0.60 mM, V_{max} = 5.833 × 10^7 M·s^{-1}	[85]
Pt-iNOS@ZIF			CAT: K_m = 172 mM, V_{max} = 3.46 × 10^{-6} M·s^{-1}	[86]
$LiMn_2O_4$	SOD, CAT, GPx, ·OH scavenging	$O_2^{\cdot-} \xrightarrow{SOD} H_2O_2 \underset{GPx}{\overset{CAT}{\rightleftharpoons}} H_2O$ $\cdot OH \xrightarrow[scavenging]{\cdot OH} H_2O$	–	[87]
RosA-Mn NPs	SOD, CAT, ·OH scavenging, RNS scavenging	$O_2^{\cdot-} \xrightarrow{SOD} H_2O_2 \xrightarrow{CAT} O_2$ $\cdot OH \xrightarrow[scavenging]{\cdot OH} H_2O$ $RNS \xrightarrow[scavenging]{RNS} NO^{2-}/NO^{3-}/N_2O\ldots$	–	[88]
Fe_3O_4-GOx	GOx, CAT, POD	$H_2O_2 \xrightarrow{POD} \cdot OH$ $GOx \rightarrow H_2O_2$; $H_2O_2 \xrightarrow{CAT} O_2$	–	[89]
mc-PDATP	SOD, GPx, POD, ·OH scavenging	$O_2^{\cdot-} \xrightarrow{SOD} H_2O_2 \xrightarrow{GPx} H_2O$ $H_2O_2 \xrightarrow{POD} \cdot OH$; $\cdot OH \xrightarrow[scavenging]{\cdot OH}$	SOD: 19.10 U·mL^{-1} POD: 70.60 U·mL^{-1} GPx: 240 U·mL^{-1}	[90]
MoS_2	SOD, CAT, GPx, POD	$O_2^{\cdot-} \xrightarrow{SOD} H_2O_2 \xrightarrow{CAT} O_2$ $GPx \rightarrow H_2O$; $H_2O_2 \xrightarrow{POD} H_2O$	GPx: K_m = 0.04 mM, V_{max} = 6.6 × 10^{-7} M·s^{-1}	[91]
ACPCAH	SOD , CAT , GOx , POD , NOS	$O_2^{\cdot-} \xrightarrow{SOD} H_2O_2 \xrightarrow{POD} O_2 \xrightarrow{iNOS} NO$ $GOx \rightarrow H_2O_2$; $H_2O_2 \xrightarrow{CAT} H_2O$	SOD: K_m = 5.26 mM, V_{max} = 3.60 × 10^{-8} M·s^{-1} CAT: K_m = 0.31 mM, V_{max} = 5.10 mg·L^{-1}·s^{-1} POD: 120 U·mg^{-1}; GOx: 119 U·mg^{-1}	[92]

(*continued on next page*)

Table 1 (*continued*)

Cascade nanozymes	Enzyme mimic	Reaction process	Kinetics	Ref
GOx@SrCaP-CAT-Tet	GOx, CAT	H_2O_2 GOx CAT O_2	–	[93]
Fe_2NC@Se	SOD, CAT, GPx, OXD	SOD $O_2^{\cdot-}$ H_2O_2 CAT GPx OXD O_2 H_2O	CAT: $K_m = 110$ mM, $V_{max} = 2.70 \times 10^{-6}$ M·s^{-1} OXD: $K_m = 1.27$ mM, $V_{max} = 2.202 \times 10^{-8}$ M·s^{-1}	[94]

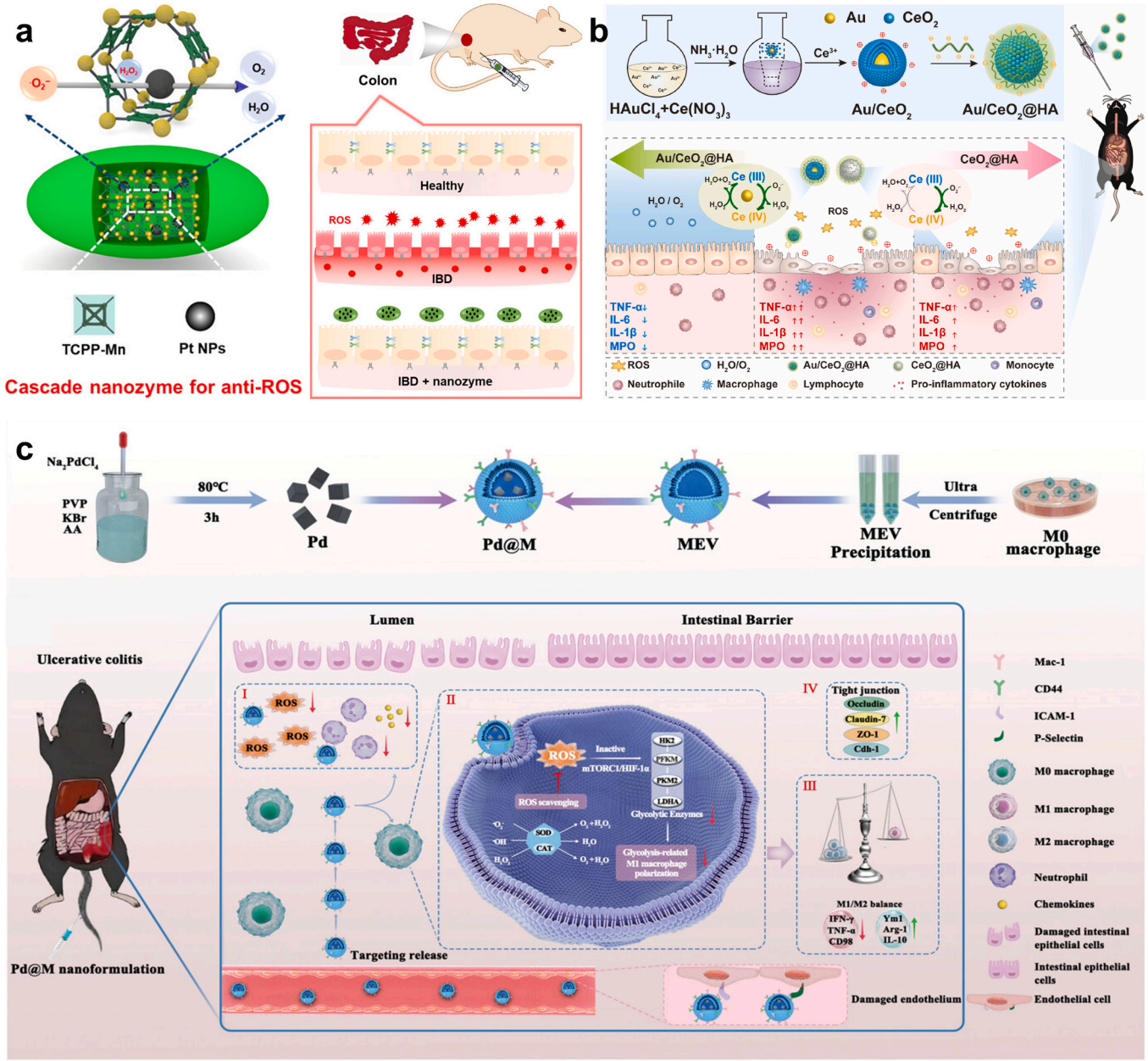

Fig. 3. Biocatalytic cascade treatment of IBD. (a) Illustration of the cascade catalysis process induced by Pt@PCN222-Mn [102]. Copyright 2020, AAAS. (b) The prepared Au/CeO_2 nanozymes for mediating SOD-CAT cascade reactions [77]. Copyright 2023, Elsevier. (c) Pd@M with multi-enzyme cascade activities to protect against UC [78]. Copyright 2023, Wiley-VCH.

innovative therapeutic strategies for IBD, harnessing the catalytic precision of nanomaterials to counteract ROS-mediated pathophysiology. Kwon et al. [100] developed a Pluronic F127-based nanocarrier co-encapsulating SOD and CAT, achieving enhanced catalytic stoichiometry through optimized enzyme ratios. This platform minimizes spatial separation between enzymes, elevating local concentrations to amplify cascade efficacy. Building on dual-enzyme coordination, Chen et al. [101] engineered a biohybrid system combining SOD-enriched *Spirulina platensis* (SP) with ceria nanoparticles (SP@COS-CeO_2). The SP's mucoadhesive glycoproteins prolong intestinal residence time, while CeO_2 acts as a CAT mimic, enabling sequential $\cdot O_2^-/H_2O_2$ elimination and hypoxia alleviation through O_2 generation. In murine models of UC and CD, SP@COS-CeO_2 exhibited significant colon-protective effects, characterized by restored epithelial architecture, tightly aligned crypts, and reduced inflammatory infiltrates compared to controls. Mechanistic analysis revealed that SP@COS-CeO_2 treatment markedly suppressed pro-inflammatory cytokine expression, with the strongest inhibition observed for TNF-α and IL-6 levels. To overcome limitations of conventional nanozymes, Wei et al. [102] biocatalytic synthesized a zirconium-based MOF (PCN222) integrating Mn(III)-porphyrin and platinum nanoparticles (Pt@PCN222-Mn) (Fig. 3a). The TCPP-Mn moiety mediates $\cdot O_2^-$ dismutation (SOD-like activity), while Pt nanoparticles catalyze H_2O_2 decomposition (CAT-like activity), as confirmed by multiple evaluation methods.

Precious metal nanoparticles have emerged as pivotal candidates for anti-inflammatory nanozyme development due to their high stability, scalable synthesis, and tunable catalytic properties. Li et al. [77] developed Au/CeO_2 nanozymes where gold nanoparticles accelerate Ce(III)/Ce(IV) cycling, enhancing SOD/CAT-like activities compared to the commercial ceria (Fig. 3b). According to the Michaelis-Menten kinetic equation for analysis, the Michaelis constant (K_m) of CAT-like activity was 3.224 mM. In the same year, Cheng et al. [78] encapsulated cubic palladium nanoparticles within macrophage-derived extracellular vesicles (Pd@M), conferring triple enzymatic activity (SOD/CAT/·OH scavenging) (Fig. 3c). The CAT enzyme kinetics results indicated that K_m and maximum reaction velocity (V_{max}) were 28.75 mM and 0.05 $mg{\cdot}L^{-1}{\cdot}s^{-1}$, respectively. MEV surface proteins (Mac-1 and CD44) mediate binding to endothelial adhesion molecules in ulcerative colitis lesions, achieving higher accumulation than non-targeted controls. Both in vitro and murine model studies demonstrated that Pd@M alleviates UC progression by remodeling the colonic immune microenvironment through suppression of glycolysis-driven M1 macrophage polarization and inflammatory cell infiltration.

Emerging developments demonstrate the inaugural application of data-driven nanomedicine design for IBD management. Systematic screening identified Ni_3S_4 [103] as an optimal synthetic nanozyme exhibiting enhanced antioxidant activity compared to natural enzymatic counterparts. This nanozyme demonstrates threefold functionality: targeted accumulation at inflamed intestinal sites, microenvironment modulation through pH-responsive action, and microbial community regulation. Comparative analyses reveal its superior acid tolerance and reactive species scavenging capacity relative to conventional therapeutics. Notably, the material's surface charge characteristics facilitate selective inflammatory targeting, while microbiota recalibration effects promote epithelial barrier restoration. These findings collectively validate Ni_3S_4 as a paradigm for rationally designed nanotherapeutics.

Wang's team [87] developed lithium-doped $LiMn_2O_4$ (LM) nanozymes through valence-state engineering, where controlled Mn oxidation (+3 → +4) optimizes simultaneous SOD, CAT, and GPx mimicry. Experimental validation confirms concentration-dependent ROS neutralization and cytokine modulation in IBD models. The valence engineering strategy elucidates structure-activity relationships governing enzymatic cascade effects, establishing a framework for multifunctional nanozyme design. Murine studies further demonstrate inflammation resolution through self-regulated redox cycles, suggesting broad applicability in inflammatory pathophysiology. In addition, in the research conducted by Muhammad et al. [104], hydrous RuO_2 were added as a template to the self-assembled gold and platinum nanoparticles (H-RuO_2@metal). Physicochemical assessments confirm superior catalytic durability and pH stability versus monometallic analogues. In established IBD murine models, these constructs significantly attenuated inflammatory mediators (IL-1β, TNF-α) while maintaining mucosal architecture.

3.2. Osteoarthritis

Osteoarthritis (OA) [105,106], a degenerative joint disorder, manifests through articular cartilage deterioration, subchondral bone remodeling, and synovial inflammation. As the predominant arthritic pathology, OA induces pain-related symptomology and functional joint impairment. Pathophysiological processes involve ROS-mediated oxidative stress [107,108], which disrupts cartilage extracellular matrix homeostasis, induces apoptotic chondrocyte death, and amplifies inflammatory cascades—collectively accelerating structural joint deterioration. The central role of ROS in OA pathogenesis has propelled therapeutic strategies focused on oxidative stress mitigation, necessitating novel nanozyme development for targeted antioxidant delivery.

Wang et al. [85] engineered a chondrocyte-targeting therapeutic platform through Mn_3O_4 nanozyme encapsulation in chondroitin sulfate (CS) hydrogels (Mn_3O_4@CS). As terminally differentiated cells central to joint metabolic homeostasis, chondrocytes in OA are prone to oxidative stress-induced damage, creating barriers for conventional drug delivery. To elucidate the antioxidative mechanism of Mn_3O_4, pharmacological inhibition with sodium diethyldithiocarbamate (SOD inhibitor) and 3-amino-1,2,4-triazole (CAT inhibitor) was employed. Experimental data confirmed the dual enzymatic capacity of Mn_3O_4 nanozymes to functionally restore SOD/CAT activities and suppress ROS-mediated inflammatory cascades. SOD exhibited a V_{max} of 4.86×10^5 $M{\cdot}s^{-1}$ and a K_m of 0.017 mM, while CAT showed a V_{max} of 5.833×10^7 $M{\cdot}s^{-1}$ with K_m of 0.6 mM. Yu et al. [109] developed a copper-based metal-organic framework (Cu MOF) nanozyme system incorporating bioinspired metal-nitrogen catalytic centers (Fig. 4a). This therapeutic platform functions through dual biological mechanisms: mitigation of HIF-1α-mediated metabolic dysregulation in chondrocytes and effective ROS elimination within synovial macrophages. Comparative assessments with copper nanoclusters and oxide counterparts revealed that Cu MOF exhibits integrated SOD/CAT enzymatic mimicry and ·OH scavenging capacity, while maintaining ROS-neutralizing specificity without generating cytotoxic intermediates. Flow cytometric analysis demonstrated comprehensive ROS subtype clearance across both cell types. Immunoblotting analysis confirmed concurrent suppression of M1 macrophage polarization markers and elevation of M2 markers, indicating complete macrophage phenotype conversion. Therapeutic validation in a collagenase-induced osteoarthritis model with high synovitis pathological features demonstrated measurable bone matrix restoration and synovitis attenuation, corroborated by OARSI histopathological scoring standards.

Guo et al. [79] established a synthetic protocol for zinc-doped mesoporous cerium oxide nanostructures (HMZC), subsequently encapsulating kartogenin (KGN) and surface-functionalizing with hyaluronic acid (HA) to yield KGN@HMZC@HA nanocomposites (Fig. 4b). Systematic antioxidant evaluations, including DPPH (2,2-diphenyl-1-picrylhydrazyl) radical quenching and $\cdot O_2^-/H_2O_2$ clearance assays, confirmed superior SOD/CAT-mimetic activities compared to conventional antioxidants. The construct demonstrates pH-sensitive therapeutic release kinetics, with enhanced payload precision under acidic conditions and minimized non-specific leakage at physiological pH. Cellular viability assessments revealed preserved membrane integrity and mitochondrial function in IL-1β-stimulated chondrocytes, alongside significant cytoprotection against cytokine-induced apoptosis. Mechanistic investigations through confocal imaging and flow cytometric ROS quantification established direct correlation between enzymatic

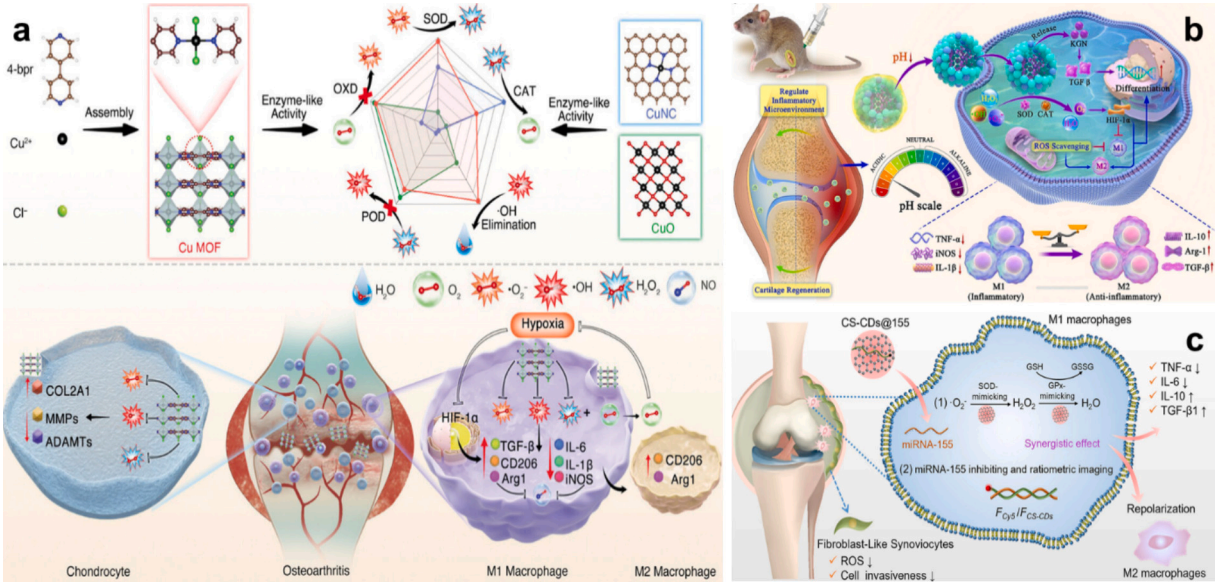

Fig. 4. Biocatalytic cascade treatment of OA and RA. (a) Illustration of cascade catalysis induced by Cu MOF [109]. Copyright 2024, Wiley-VCH. (b) KGN@HMZC@HA nanocomposites with multi-enzyme cascade activities to protect against OA [79]. Copyright 2024, Elsevier. (c) Schematic illustrating the production and use of CS-CDs@155 [110]. Copyright 2024, Elsevier.

antioxidant capacity and cellular protection. In vivo evaluations further demonstrated multifaceted therapeutic actions including oxygen generation, macrophage polarization modulation, and pH-dependent chondroprotection through controlled KGN release.

3.3. *Rheumatoid arthritis*

Rheumatoid arthritis (RA) [111,112] is characterized as a chronic autoimmune pathology involving sustained synovial inflammation and progressive articular destruction. This disorder predominantly impacts metacarpophalangeal and metatarsophalangeal joints, manifesting as progressive articular pain, edema, and structural deformation. ROS-mediated oxidative stress [113,114] constitutes a fundamental pathomechanism in RA progression, establishing oxidative stress modulation as a strategic therapeutic target.

Gong et al. [110] developed cerium/selenium-co-doped carbon quantum dots (CS-CDs) functionalized with anti-miRNA-155 oligonucleotides (CS-CDs@155) to reverse macrophage polarization from M1 to M2 phenotypes, effectively disrupting the ROS-inflammatory feedback loop in RA pathogenesis (Fig. 4c). The engineered nanocomposites demonstrated dual enzymatic functionality through cerium-mediated SOD mimicry and selenium-dependent GPx activity. Comprehensive antioxidant evaluations—including salicylate trapping assays, glutathione redox cycling analyses, and $ABTS^{+}$ (2,2′-azino-bis(3-ethylbenzothiazoline-6-sulfonic acid)) radical neutralization tests—verified cascade ROS elimination capacity targeting $\cdot O_2^-$, H_2O_2, and ·OH. Cellular protection was evidenced by substantially reduced apoptosis rates (13.06 % vs 61.12 % in controls). Immunochemical analyses revealed concurrent downregulation of pro-inflammatory mediators (TNF-α, IL-6) and elevation of anti-inflammatory cytokines (IL-10, TGF-β1). Therapeutic administration in arthritic models demonstrated 82.3 % reduction in paw edema volume, attenuated synovial hyperplasia, and diminished leukocyte infiltration compared to conventional treatments.

Jia et al. [115] developed a biomimetic delivery platform (MMV-MnO_2@DSP) by integrating manganese dioxide nanoparticles (MnO_2) and dexamethasone sodium phosphate (DSP) into macrophage-derived microvesicles (MMVs) for multi-mechanistic RA therapy. This nanosystem combines dual SOD/CAT-mimetic activities with MMV's innate synovial-targeting capability: MnO_2 cascades $\cdot O_2^-$ to H_2O_2 and subsequently to H_2O and O_2, while MMVs facilitate inflammatory joint homing. Ultrathin-section transmission Ultrathin-section TEM analysis demonstrated successful lysosomal evasion and cytoplasmic predominance in activated macrophages. Immunofluorescence and Western blot analyses demonstrated significant downregulation of TNF-α and IL-1β expression. Near-infrared II in vivo imaging revealed that MMV-MnO_2@DSP was enriched more in the joint area than in the free drug group in RA model mice and had a longer half-life in circulation. Further micro-computed tomography (Micro-CT) studies have shown that the MMV-MnO_2@DSP treatment group significantly alleviated synovial hyperplasia, inflammatory cell infiltration, and bone and cartilage destruction. By synergizing vesicle-mediated targeting with nanozyme catalytic detoxification, this study successfully disrupted the pro-inflammatory TLR/NF-κB positive feedback loop, establishing a novel paradigm for precise RA therapy.

Although intra-articular administration of anti-inflammatory agents constitutes current clinical interventions, inherent limitations including iatrogenic infection risks from frequent injections and absence of disease-modifying capabilities remain unresolved. To overcome these therapeutic constraints, He et al. [83] developed an injectable bioadhesive hydrogel system integrating three functional components: a dopamine-modified hyaluronic acid (DA-HA) matrix, sulfated hyaluronic acid (SO_3-HA) networks, and kartogenin-conjugated copper single-atom nanozymes supported on dopamine-functionalized graphene quantum dots (DAGQD@Cu@KGN SAN). The composite hydrogel concurrently demonstrated triple-enzymatic antioxidant activities (SOD, CAT, ·OH scavenging) for inflammation suppression and chondroprotective lubrication restoration. Cellular assays confirmed significant downregulation of pro-inflammatory cytokines (TNF-α, IL-6) and upregulation of IL-10. Furthermore, the construct mediated efficient recruitment of bone marrow-derived mesenchymal stem cells to defect regions. Transcriptomic profiling identified Foxo antioxidant pathway activation alongside concurrent inhibition of lysosomal activation pathways, osteoclast differentiation markers, and TNF signaling cascades. In collagen-induced arthritis models, treated joints displayed preserved chondral morphology and pronounced upregulation of cartilage-specific markers (Sox9, Collagen II, Aggrecan) relative to control cohorts. This engineered platform exhibits multimodal therapeutic efficacy through integrated anti-inflammatory action and tissue regeneration, representing a paradigm shift in RA management.

3.4. Diabetic complication

The pathophysiological implications of diabetes mellitus (DM) have garnered significant attention within biomedical research communities. DM represents a metabolic disorder characterized by dysregulated glucose homeostasis, which is commonly associated with multifactorial complications including but not limited to cutaneous ulceration and systemic inflammatory manifestations [116,117]. Emerging evidence suggests that the pathogenesis of these complications exhibits substantial correlation with elevated oxidative stress levels, predominantly mediated by excessive ROS production The therapeutic potential of antioxidants lies in their capacity to effectively scavenge ROS, thereby mitigating oxidative tissue damage and associated pathological cascades.

Du et al. [89] have developed and investigated a pH-responsive nanozyme system employing Fe_3O_4-GOx composite nanoparticles for diabetic ulcer management. Their research demonstrates an engineered nanozyme system integrating iron oxide nanoparticles with glucose oxidase encapsulation, designed specifically for wound microenvironment modulation. This composite nanozyme concurrently demonstrates dual-enzyme cascade functionalities (GOx/POD and GOx/CAT) with pH-dependent catalytic switching behavior. Systematic evaluation of pH effects on peroxidase-nanozyme cascade catalysis (PNCC) revealed optimal oxygen generation under neutral (pH 7.5) and mildly acidic (pH 6.5) conditions, facilitating efficient GOx/CAT cascade activation. Comparative analysis of TMB oxidation demonstrated superior GOx/POD catalytic efficiency at pH 5.5–6.5. This pH-modulated behavior establishes oxygen flux regulation through cascaded enzymatic reactions as the principal therapeutic mechanism. In murine models of MRSA-infected diabetic ulcers, the Fe_3O_4-GOx treatment cohort exhibited accelerated wound epithelialization rates, achieving complete biofilm eradication within 15 days - representing a clinically significant reduction in wound closure duration. Comprehensive biosafety assessments confirmed the system's biocompatibility and non-cytotoxic profile. Notably, this oxygen-economical therapeutic platform outperforms conventional phototherapy approaches through three distinctive advantages: illumination-independent antimicrobial efficacy, pH-responsive bactericidal activity optimized for wound pH fluctuations, and enhanced angiogenesis promotion.

The pathologically hyperglycemic and chronically inflamed microenvironment characterizing diabetic foot ulcers (DFU) [118,119] contributes to the exacerbation of tissue hypoxia, perpetuation of inflammatory cascades, and impaired wound healing processes. Addressing this clinical challenge, Shang et al. [92] engineered a multifunctional therapeutic platform (ACPCAH) comprising co-encapsulated L-arginine, ultrasmall gold nanoparticles, and $Cu_{1.6}O$-decorated phosphorus-doped graphitic carbon nitride nanosheets within a hydrogel spray matrix, specifically designed for DFU management (Fig. 5a). This tripartite nanocomposite achieves simultaneous implementation of SOD, CAT, GOx, POD, and nitric oxide synthase (NOS)-mimetic cascade systems. Dynamic enzymatic data reveal the following kinetic parameters: SOD exhibits a K_m of 5.26 mM and V_{max} of 3.6×10^{-8} $M{\cdot}s^{-1}$; for CAT, the K_m is 0.31 mM with a V_{max} of 5.1 $mg{\cdot}L^{-1}{\cdot}s^{-1}$. Additionally, the GOx-like activity of ACPCAH is measured at 119 $U{\cdot}mg^{-1}$. This system primarily facilitates the regulation of enzyme activity through microenvironmental pH changes. Both in vitro and in vivo wound healing experiments have demonstrated that ACPCAH exhibits enhanced antibacterial activity under ultrasound compared to the control group. Furthermore, it significantly upregulates the expression of angiogenic growth factors in wound tissues, promotes wound healing, and suppresses inflammation by depleting excess glucose at the wound site.

Diabetic complications encompass more complex pathophysiology than conventional chronic wound management, with diabetic osteoporosis (DOP) [120–122] constituting a significant yet unresolved comorbidity marked by progressive trabecular microstructure deterioration. Contemporary DOP management strategies predominantly depend on antihyperglycemic pharmacotherapy or bisphosphonates, both constrained by treatment-limiting toxicities including gastrointestinal complications and medication-related osteonecrosis, highlighting the urgent requirement for safer therapeutic alternatives. Addressing this therapeutic gap, Fu and colleagues [93] developed a bone-homing enzymatic nanocomposite (GOx@SrCaP-CAT-Tet) through tetracycline-conjugated strontium-substituted calcium phosphate nanoparticles co-encapsulating GOx and catalase CAT (Fig. 5b). This system functions through dual metabolic coordination: enzymatic tandem catalysis (GOx-CAT) mediating localized glucose depletion and subsequent H_2O_2 neutralization, thereby alleviating hyperglycemic

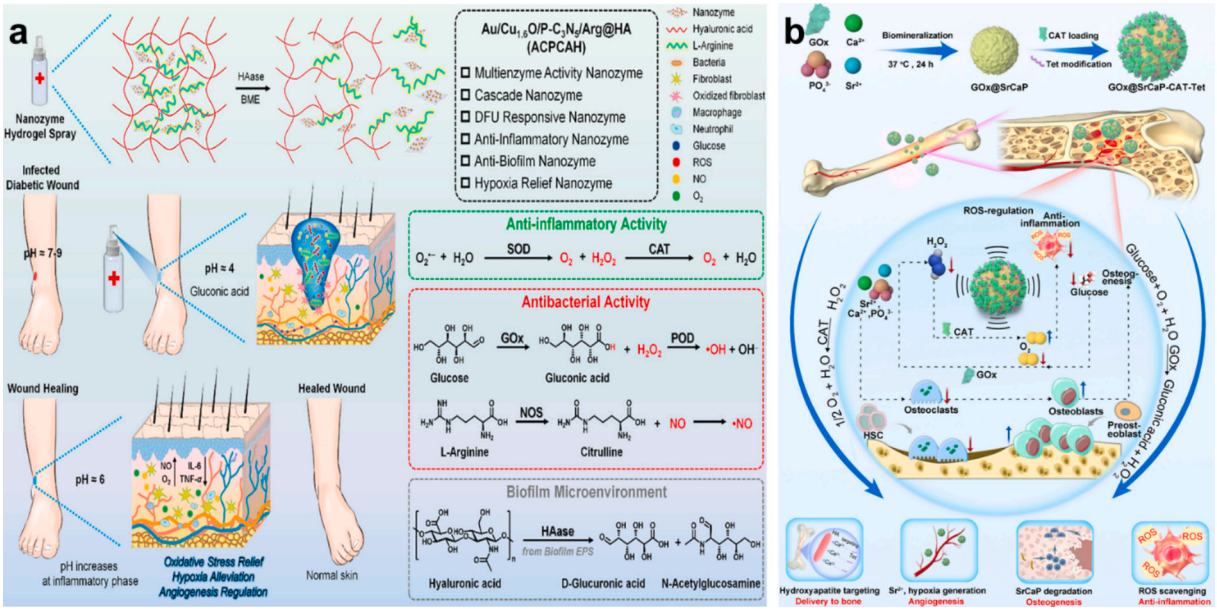

Fig. 5. Biocatalytic cascade treatment of diabetic complication. (a) Illustration of ACPCAH bearing SOD-CAT-GOx-POD-NOS cascade activities for DFU therapy [92]. Copyright 2023, American Chemical Society. (b) Schematic illustration of GOx@SrCaP-CAT-Tet mimicking GOx-CAT cascade catalytic reactions for DOP therapy [93]. Copyright 2025, American Chemical Society.

oxidative stress; Sustained Sr^{2+} release from biodegradable SrCaP matrices activates calcium-sensing receptors (CaSR), creating osteoinductive microenvironments via HIF-1α-mediated angiogenesis and osteogenic differentiation.

3.5. Liver ischemia-reperfusion injury

Liver ischemia-reperfusion injury (IRI) constitutes a multifaceted pathological process involving intricate molecular interactions, with ROS serving as pivotal mediators. Under ischemic conditions [123,124], cellular metabolic homeostasis becomes severely compromised. Subsequent reperfusion paradoxically exacerbates tissue damage through abrupt oxygen reintroduction, precipitating uncontrolled ROS generation that overwhelms endogenous antioxidant defenses. Mu and colleagues [86] developed an innovative hybrid nanoreactor (Pt-iNOS@ZIF) through precise integration of zeolitic imidazolate framework-8 (ZIF-8) matrices with ultrafine platinum nanoparticles (Pt NPs) and inducible nitric oxide synthase (iNOS), thereby conferring dual

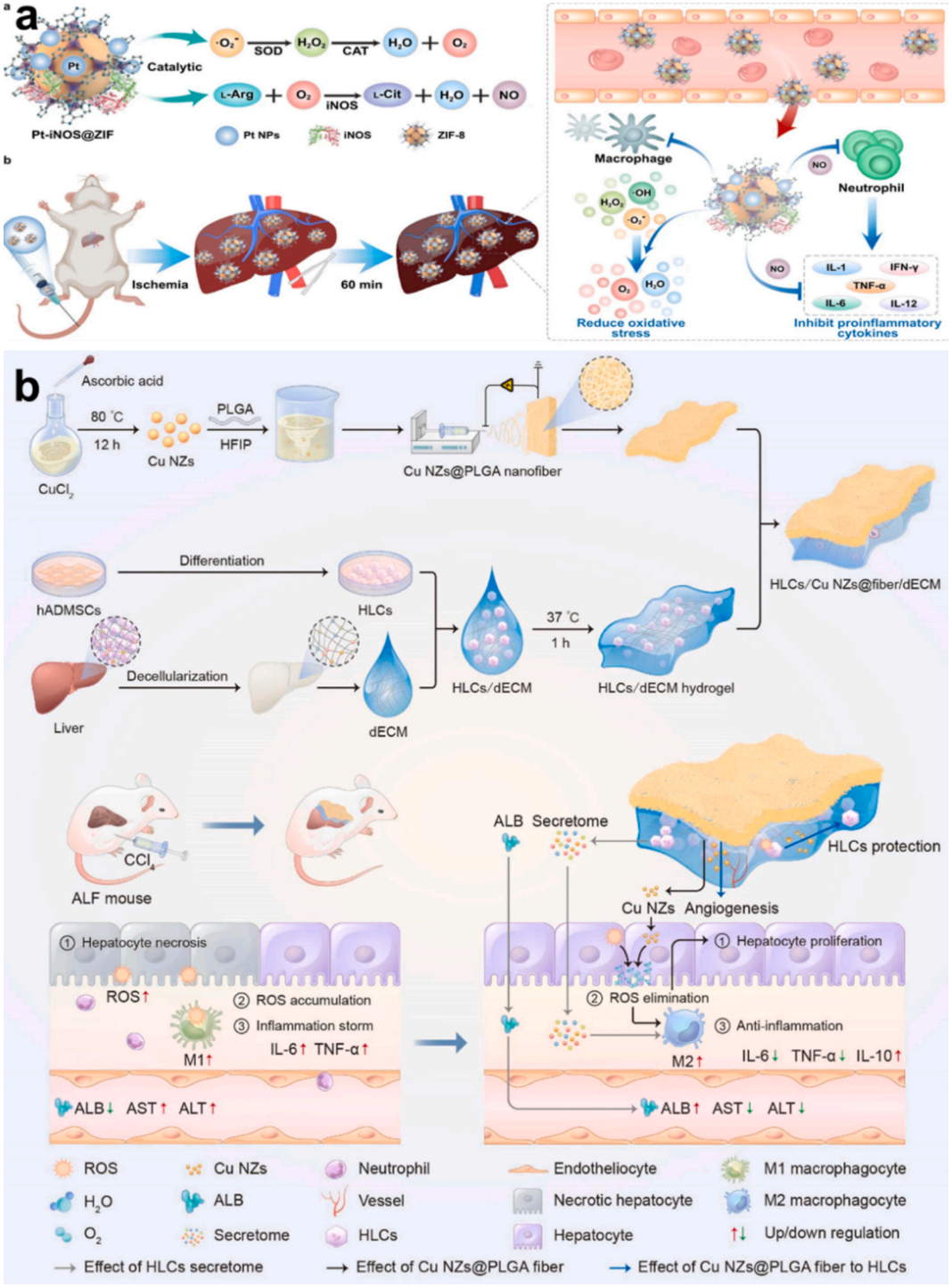

Fig. 6. Biocatalytic cascade treatment of liver IRI. (a) Schematic illustration of hepatic IRI prevention performance by Pt-iNOS@ZIF nanoreactor bearing SOD-CAT-iNOS cascade reactions [86]. Copyright 2022, Springer Nature. (b) Illustration of the prepared HLCs/Cu NZs@fiber/dECM platform for ALF therapy [125]. Copyright 2023, Elsevier.

functionality through biomimetic SOD and CAT activities (Fig. 6a). The Michaelis-Menten curves and linewewe-Burk plot obtained K_m and V_{max} as 172 mM and 3.46 × 10^{-6} M·s^{-1}, respectively This multifunctional nanoplatform effectively attenuated hepatic IRI through concerted ROS neutralization and NO-dependent cytoprotective mechanisms. Enzymatic characterization demonstrated enhanced catalytic performance relative to native enzymes. Quantitative antioxidant assessment via $ABTS^+$ radical elimination confirmed the material's superior free radical scavenging capacity. Biodistribution analysis revealed preferential hepatic accumulation, correlating with significant attenuation of serum hepatic injury biomarkers. Of particular note, Pt-iNOS@ZIF administration at 2 mg/kg achieved comparable therapeutic outcomes to the clinical benchmark *N*-acetylcysteine (150 mg/kg), concurrently mitigating inflammatory responses through suppression of macrophage activation and neutrophil recruitment. Mechanistic investigations employing transcriptomic analysis identified coordinated downregulation of pro-inflammatory mediators (TNF-α, IL-6) and IL-10 upregulation via NF-κB/MAPK signaling modulation. These collective findings establish Pt-iNOS@ZIF as a transformative nano-therapeutic strategy for targeted management of IRI-related pathophysiology.

3.6. Liver fibrosis

Hepatic fibrosis represents a pathological progression marked by excessive extracellular matrix protein deposition, culminating in structural scarring and progressive hepatic dysfunction. Pathologically elevated ROS levels perpetuate oxidative stress cascades that exacerbate hepatocyte injury, inflammatory responses [126–128], and activation of hepatic stellate cells - primary mediators of fibrogenesis. This redox imbalance critically amplifies fibrotic progression, underscoring ROS-mediated oxidative damage as a fundamental pathogenic driver in fibrotic initiation and advancement. Molybdenum disulfide (MoS_2) nanomaterials have recently gained prominence in biomedical contexts due to their favorable biocompatibility profile and inherent multi-enzymatic catalytic properties. Building upon these intrinsic characteristics, Zhang et al. [91] conducted comprehensive investigations into the enzymatic cascade mechanisms and antioxidant potential of MoS_2 nanozymes. Their systematic analysis demonstrated pan-reactive oxygen species elimination capacity through simultaneous SOD, CAT, POD, and GPx-mimetic activities. The determined kinetic parameters for GPx include K_m of 0.04 mM and V_{max} of 6.6 × 10^{-7} M·s^{-1}. Notably, the pH-dependent catalytic transition facilitated selective H_2O_2 decomposition within acidic lysosomal microenvironments (pH 4.5–5.5), thereby achieving localized oxidative stress mitigation and enhanced anti-inflammatory responses. In experimental hepatic fibrosis models, MoS_2 nanosheets administration significantly ameliorated histopathological manifestations, including inflammatory cell infiltration reduction and hepatic parenchymal architecture preservation. Concomitant serum biomarker evaluations provided biochemical validation of therapeutic efficacy, demonstrating reduced HA and IL-1β levels indicative of systemic inflammation attenuation. These findings collectively establish MoS_2 nanosystems as scientifically substantiated candidates for catalytic therapeutic intervention in oxidative stress-associated fibrotic disorders.

Hepatic fibrosis and acute liver failure (ALF) [129,130] maintain a pathophysiologically intertwined relationship, wherein fibrosis constitutes a critical transitional phase predisposing to end-stage hepatic decompensation upon uncontrolled progression. Progressive fibrotic remodeling disrupts lobular architecture and metabolic homeostasis, ultimately precipitating ALF through cumulative functional deterioration. ROS-mediated oxidative stress not only potentiates hepatic injury but also drives fibrotic advancement through functional hepatocyte impairment and accelerated extracellular matrix deposition. Jin et al. [125] recently developed an innovative composite therapeutic system (HLCs/Cu NZs@fiber/dECM) comprising copper oxide nanozyme-functionalized PLGA nanofibers integrated with decellularized extracellular matrix hydrogels for ALF management. The engineered nanozymes demonstrated multispectrum ROS neutralization capacity through efficient elimination of $\cdot O_2^-$, ·OH, and H_2O_2, effectively disrupting oxidative stress amplification during early ALF pathogenesis (Fig. 6b). The Cu NZs-incorporated PLGA nanofibrous scaffolds conferred cytoprotective effects via ROS scavenging and enhanced hepatocyte viability under oxidative duress. Mechanistic investigations revealed macrophage polarization shift toward regenerative M2 phenotypes, as quantified by transcriptional suppression of pro-inflammatory cytokines (TNF-α, IL-1β) and concurrent IL-10 elevation in treated hepatocytes. Murine ALF models demonstrated full functional recovery, evidenced by complete normalization of serum albumin (ALB) and aminotransferase levels within seven days post-intervention. Histomorphological evaluations confirmed near-complete parenchymal restoration with diminished presence of oxidative damage markers, apoptotic indices, or necrotic zones. Whole-transcriptome analysis validated therapeutic mechanisms through coordinated downregulation of inflammatory regulators (IL-33, HIF-1α) and sustained activation of antioxidant defense systems (SOD1, SOD2, GPX) coupled with angiogenic induction (VEGFA overexpression).

3.7. Acute kidney injury

Acute kidney injury (AKI), clinically defined by a rapid decline in renal filtration capacity, arises from multifactorial pathogenic stimuli, including ischemia, nephrotoxic insults, and systemic inflammatory cascades. A key pathological feature of AKI is the surge in ROS [131,132], which induces mitochondrial dysfunction, exacerbates cellular bioenergetic collapse, and potentiates apoptotic and necrotic cell death pathways. Addressing this therapeutic void, Yang et al. [133] developed a metal-organic cage derivative (MOC-—O) incorporating pyridine nitrogen oxide moieties that demonstrate sequential SOD/CAT catalytic cascades for targeted ROS elimination in AKI (Fig. 7a). In vitro assessments demonstrated the favorable biocompatibility profile of —MOC-O, along with its potent ROS scavenging capacity in HK-2 renal proximal tubule cells. In vivo studies using a murine model of AKI demonstrated that MOC-O can effectively accumulate in the injured kidney due to its ultrasmall size and the presence of an incomplete endothelial barrier.

Sahu et al. [134] constructed a heparin-conjugated cascade nanozymes system (—Hep-H) through precision integration of hemin chloride nanoparticles, which recapitulate complementary SOD- and CAT-like enzymatic functions. Comparative enzymatic analysis revealed that Hep-H nanozymes maintained superior SOD-like activity, retaining over 70 % $\cdot O_2^-$ neutralization efficiency after 14-day incubation. In murine cisplatin-induced AKI models, real-time fluorescence tracking demonstrated preferential renal biodistribution with enhanced fluorescence signal retention in pathologically compromised versus healthy renal tissue. Therapeutic outcomes were corroborated by marked reductions in blood urea nitrogen (BUN) and serum creatinine (CRE) levels, concomitant with diminished kidney injury molecule-1 (KIM-1) expression in renal parenchyma. Histomorphometric analysis further evidenced significant mitigation of oxidative damage indices and inflammatory infiltrates, collectively substantiating the system's robust therapeutic potential through dual antioxidative and anti-inflammatory modulation.

As nanozyme-mediated antioxidant therapy emerges as a promising strategy for modulating redox homeostasis, its clinical translation remains constrained by suboptimal renal targeting efficiency and dose-dependent systemic toxicity. To address these challenges, Yuan et al. [88] developed a metal-phenolic cascade nanozymes (RosA-Mn NPs) integrating SOD-like and CAT-like activities, specifically designed for AKI management (Fig. 7b). At a catalytic concentration of 30 μg/mL, RosA-Mn NPs achieved 70 % scavenging efficiency against $ABTS^+$ and DPPH radicals, with SOD-like activity reaching 100 % equivalence to natural enzymes. TEM revealed that RosA-Mn NPs restored mitochondrial cristae architecture in oxidatively stressed renal tubular cells.

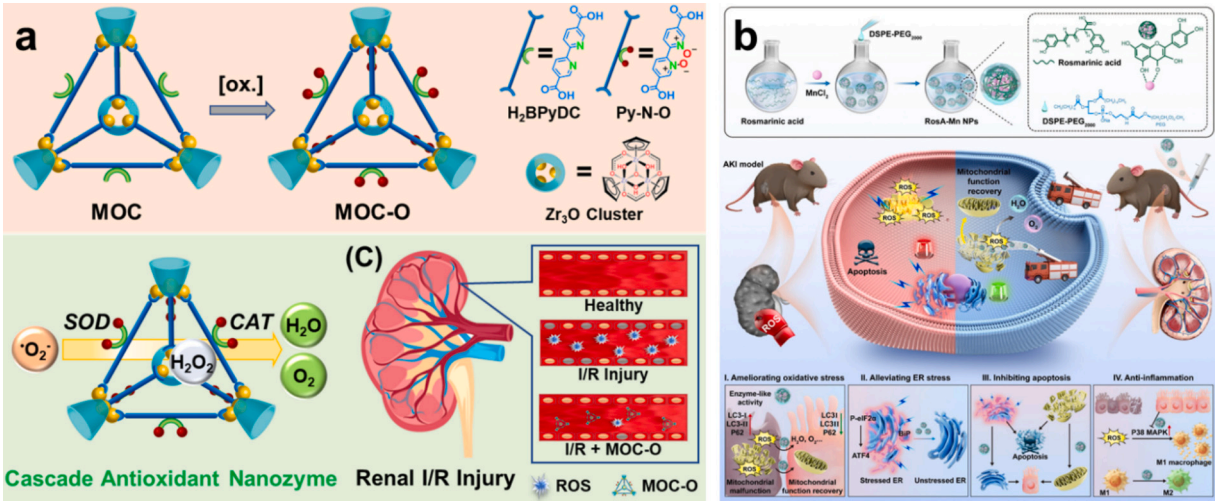

Fig. 7. Biocatalytic cascade treatment of AKI. (a) Illustration of the preparation and cascade catalytic process of MOC-O for renal I/R injury [133]. Copyright 2024, Royal Society of Chemistry. (b) Schematic representation of RosA-Mn NPs for the Treatment of AKI [88]. Copyright 2023, American Chemical Society.

Transcriptomic profiling via qRT-PCR demonstrated a 20-fold downregulation of pro-inflammatory mediators TNF-α and CXCL10 in LPS-activated macrophages, disrupting the ROS-NF-κB feedforward loop implicated in AKI progression. In a murine cisplatin-induced AKI model, RosA-Mn NPs mitigated systemic inflammation, reducing serum levels of TNF-α, IL-6, IL-1β, and IFN-γ compared to untreated controls. This multifunctional nanozyme platform represents a paradigm shift in precision antioxidant therapy, synergistically addressing oxidative stress, inflammation, and mitochondrial dysfunction in AKI pathophysiology. Wu et al. [90] engineered a multifunctional antioxidant nanozyme (mc-PDATP) incorporating dopamine motifs, tailored to combat renal oxidative damage through synergistic ROS scavenging. This nanozyme exhibited robust enzymatic mimicry, demonstrating SOD-like, POD-like, and GPx-like activities. The measured enzymatic activities were as follows: SOD at 19.1 U·mL^{-1}, POD at 70.6 U·mL^{-1}, and GPx at 240 U·mL^{-1}. In a murine model of cisplatin-induced acute kidney injury (AKI), mc-PDATP treatment restored renal functional biomarkers—including CRE and BUN—and significantly downregulated the expression of neutrophil gelatinase-associated lipocalin (NGAL) and KIM-1. These findings position mc-PDATP as a promising therapeutic candidate for precision nanotherapy in the treatment of ROS-driven nephropathy.

3.8. Myocardial injury

Myocardial injury (MI) [135,136] frequently precipitated by ischemic events, myocardial infarction, or chronic cardiac pathologies, is intricately linked to oxidative stress and the overproduction of ROS. Elucidating the interplay between MI and ROS is pivotal for devising efficacious therapeutic interventions. Xiang et al. [80] introduced a novel platform with multifaceted enzyme-mimicking activities, termed MOF-based nanozyme (denoted as Cu-TCPP-Mn), designed to emulate natural antioxidant systems for MI management. The authors demonstrated that the reversible one-electron redox cycling between Mn(III) and Mn(IV) confers sequential SOD-like and CAT-like cascade activities (Fig. 8a). Notably, the apparent affinity of Cu-TCPP-Mn (K_m = 34.65 mM, V_{max} of 0.01 mg·L^{-1}·s^{-1}) surpasses that of native CAT. Experimental findings revealed that the bimetallic active site within Cu-TCPP-Mn effectively mitigates inflammatory damage and attenuates ventricular remodeling. Compared with untreated controls, Cu-TCPP-Mn nanozyme administration significantly diminished ROS levels in ischemic myocardium and curtailed cardiomyocyte apoptosis. To further investigate its cardioprotective efficacy, postoperative cardiac remodeling was assessed in MI mouse models. Results indicated a marked reduction in scar tissue size, accompanied by decreased fibrosis and improved cardiac morphology.

3.9. Ischemic stroke

The contemporary definition of ischemic stroke (IS) encompasses an abrupt disruption in cerebral blood flow, precipitating rapid neuronal dysfunction. This condition may arise from either ischemic occlusion due to thromboembolic events or hemorrhagic rupture of cerebral vessels. The incidence and severity of stroke exhibit a pronounced correlation with advancing age, hypertension, diabetes mellitus, and lifestyle-associated risk factors [137,138]. Elevated ROS levels contribute to oxidative stress, which exacerbates neuronal injury during the acute phase and subsequent recovery period [139]. This interplay highlights the pivotal role of ROS in stroke pathophysiology and underscores the imperative for targeted therapeutic strategies to mitigate oxidative damage and enhance clinical outcomes.

Recently, the emergence of single-atom nanozymes has garnered significant attention owing to their exceptional catalytic activity and selectivity. Tian et al. [94] reported a transformative advancement through the development of a multifunctional antioxidant platform (Fe_2NC@Se), comprising dual-iron-atom nanozymes (Fe_2NC) encapsulated within selenium-doped metal-organic framework (Se-MOF) shells. Comprehensive theoretical investigations and steady-state kinetic analyses revealed that Fe_2NC exhibits triple-enzyme mimetic activities—SOD, CAT, and OXD—while the Se-MOF shell confers GPx-like functionality. Kinetic analysis reveals that the CAT exhibits K_m of 0.11 M and V_{max} of 2.70 × 10^{-6} M·s^{-1}, while the oxidase (OXD) shows K_m of 1.27 M and V_{max} of 22.02 nM·s^{-1}. The synergistic effect of SOD-like, CAT-like, and OXD-like activities demonstrates a highly effective capacity in reducing intracellular ROS following IS. Biocompatibility assessments via CCK-8 assays and laser confocal microscopy demonstrated the excellent cytocompatibility of Fe_2NC@Se. Flow cytometric analysis post-treatment revealed a substantial reduction in apoptotic cell populations, corroborated by live/dead fluorescence staining assays showing dose-dependent increases in viable cell density. Collectively, these findings validate the nanocomposite's capacity to attenuate oxidative stress-induced cellular damage. Mechanistically, Western blot analysis elucidated that Fe_2NC@Se modulates apoptotic pathways through dose-responsive upregulation of the anti-apoptotic protein Bcl-2 and concurrent downregulation of the pro-apoptotic effector Bax. In a middle cerebral artery occlusion rat model, Fe_2NC@Se demonstrated robust neuroprotective efficacy, as evidenced by quantitative histochemical analyses revealing reduced cerebral infarct volumes and diminished lipid peroxidation markers. Furthermore, the nanozyme

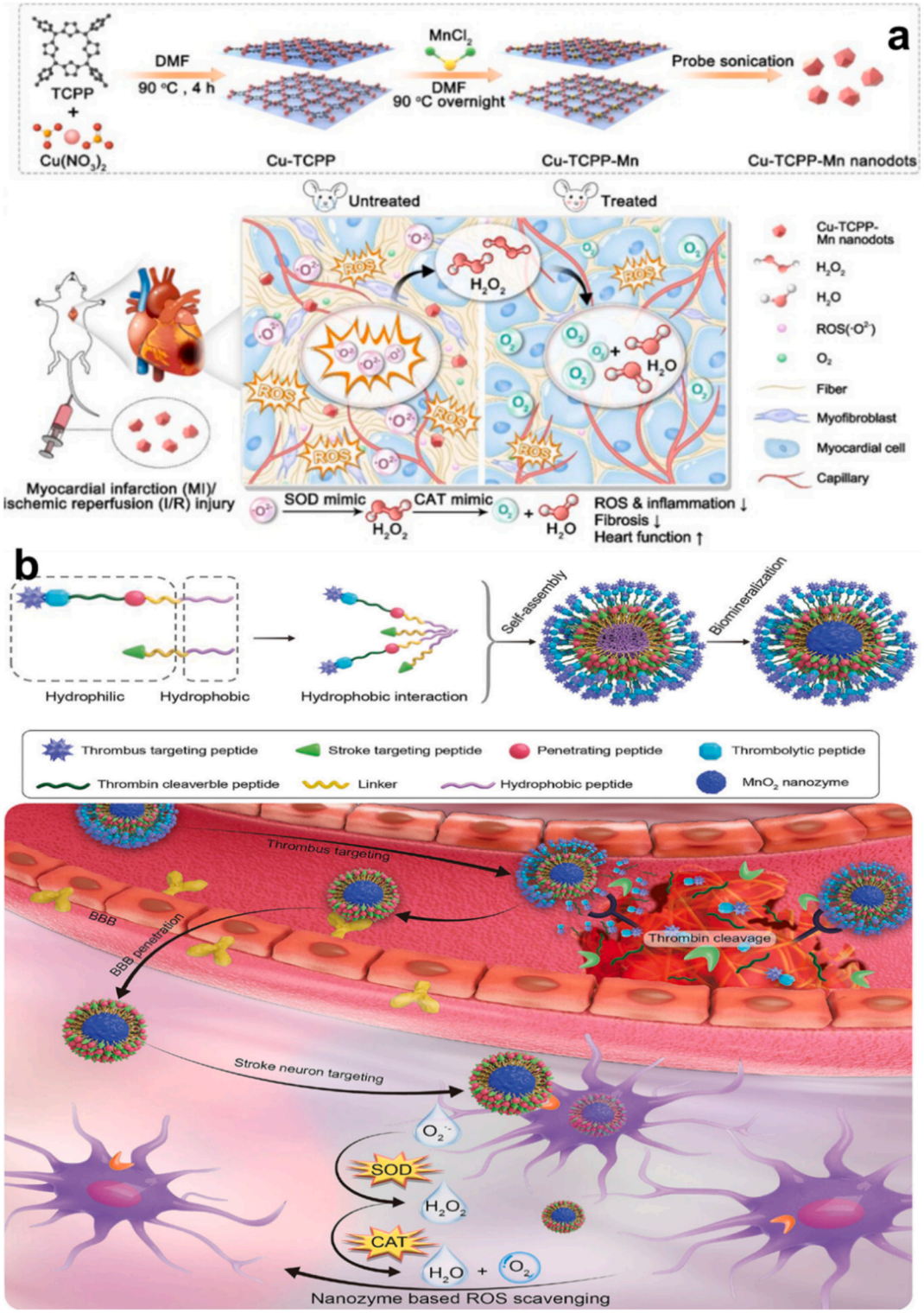

Fig. 8. Biocatalytic cascade treatment of cardiovascular and cerebrovascular diseases. (a) Schematic illustration of the design and synthesis of Cu-TCPP-Mn nanozyme for myocardial injury treatment [80]. Copyright 2023, Ivyspring International Publisher. (b) Illustration of the synthetic procedure of PNzyme/MnO_2 for Ischemic stroke therapy [81]. Copyright 2023, Wiley-VCH.

significantly suppressed phosphorylation of apoptosis signal-regulating kinase 1 (p-ASK1) and c-Jun N-terminal kinase (p-JNK), key mediators of oxidative stress-induced apoptosis, thereby ameliorating ischemia-reperfusion injury through multimodal antioxidant and anti-apoptotic mechanisms.

Wang et al. [81] engineered a polypeptide-templated manganese dioxide nanozyme (PNzyme/MnO_2) for targeted intervention in IS (Fig. 8b), exhibiting dual therapeutic efficacy in alleviating cerebral ischemic injury and modulating neuroinflammatory responses. Catalytic characterization demonstrates that PNzyme/MnO_2 exhibits intrinsic SOD-like and CAT-like activities, accompanied by superior kinetic parameters. Specifically, it shows a SOD-like activity of 2139.86 ± 234.90

U·mg^{-1}, a CAT-like activity of 255.77 ± 17.43 U·mg^{-1}, K_m of 4.9±0.99 mM, and V_{max} of (5.22±0.23) × 10^{-2} M·s^{-1}. Notably, this nanozyme exhibits exceptional blood-brain barrier (BBB) penetrability, enabling precise accumulation in ischemic brain regions while effectively suppressing astrocyte activation and pro-inflammatory cytokine release. In middle cerebral artery occlusion models, PNzyme/MnO_2 achieved a 41.3 % reduction in infarct volume and a 2.1-fold improvement in neurological scores compared to the clinical standard therapy, with concurrent BBB traversal verified by in vivo imaging. Mechanistic investigations further elucidated its capacity to downregulate pro-apoptotic Bax while upregulating anti-apoptotic Bcl-2, synergistically mitigating oxidative stress-induced neuronal apoptosis. These multimodal functionalities position PNzyme/MnO_2 as a transformative therapeutic platform for cerebrovascular pathologies.

3.10. Neuroinflammation

Neuroinflammation and oxidative stress, serving as key markers of neurodegenerative diseases, can exacerbate disease progression [140–142]. Consequently, identifying treatment strategies that target the interplay between ROS and these markers becomes critically important. Notably, composite nanoparticles play an increasingly interesting role in therapy. Based on this, Gao et al. [84] developed a nanocomposite, PMC NPs, PEI-Mn nanoparticle loading curcumin (PEI-Mn@curcumin), exhibit specific SOD-like and CAT-like activities for neuroinflammation. By taking advantage of the antioxidant activity of Mn^{3+}/Mn^{2+} redox pairs and curcumin, the pro-inflammatory cytokines TNF-α and iNOS are downregulated, while the anti-inflammatory cytokine IL-10 is upregulated, thereby alleviating intracellular oxidative stress. Cytocompatibility and blood compatibility tests showed that PMC NP had acceptable biocompatibility. For the antioxidant and cell protective functions, PMC NP showed higher viability, maintaining 80 % cell viability even at a concentration of 400 μM H_2O_2. In the protein level experiment, PMC NPs group showed better anti-inflammatory effect compared with PEI-Mn group and curcumin group, because it can downregulate the pro-inflammatory cytokines TNF-α and iNOS, and upregulate the anti-inflammatory cytokine IL-10.

3.11. Spinal cord injury

Spinal cord injury (SCI) [143–145] induces substantial neurological deficits and is associated with various complications, including inflammation and neurodegeneration. A pivotal aspect of SCI pathology involves the role of ROS, which contribute to secondary injury mechanisms. Xiong et al. [82] introduced a multifunctional nanozyme, $^{IRF\text{-}5}$SiRNA@pMn, integrating valence-engineered Mn_3O_4 nanoparticles and "pollen"-shaped $^{IRF\text{-}5}$SiRNA for a combinatorial antioxidant and anti-inflammatory therapeutic strategy in SCI. The Mn_3O_4 nanozyme mediates an efficient catalytic cascade through the integration of SOD-, CAT-, and GPx-mimetic activities. The K_m of CAT and GPx of the nanozyme were 48.13 and 71.36 mM. The V_{max} were determined to be 17.09 M·s^{-1} for CAT and 4.701 M·s^{-1} for GPx. It synergistically converts elevated reactive oxygen species (ROS) into molecular oxygen, thereby alleviating oxidative stress while promoting angiogenesis. Simultaneously, this system inhibits the NF-κB inflammatory signaling pathway and reduces macrophage-mediated production of pro-inflammatory cytokines. To prevent compensatory inflammatory escalation, the platform incorporates interferon regulatory factor 5 (IRF-5)-targeting small interfering RNA (siRNA), which is delivered via pollen-shaped nanocarriers and effectively suppresses IRF-5 expression. Consequently, the system reprograms macrophage polarization by blocking the transition from M0/M2 to M1 phenotypes, ultimately resolving the underlying inflammatory pathogenesis.

4. Conclusion

Cascade nanozymes take advantage of their high atomic economy, few by-products and low energy consumption, and coordinate multiple enzyme-catalyzed cascade reactions with spatio-temporal precision for the treatment of aseptic inflammatory diseases. The cascade mechanism allows multiple components to maintain their functional activities following stimulus initiation. This enables close integration and improved coordination among diverse therapeutic modalities, thereby enhancing treatment efficacy through synergistic interactions. The involved biocatalysis cascade reactions include five types: linear, orthogonal, parallel, cyclic and triangular cascade, among which the first three are the most widely developed and applied. In addition to the therapeutic effect being concerned, people are also concerned about whether the biological safety [146–148] of these nanozymes in vivo can be guaranteed. For these nanozymes, the body has multiple mechanisms to eliminate them [149], such as excreting them through the kidneys, decomposing them by enzymes in the liver, or identifying and eliminating them through the immune system. Current research on complex metabolic networks remains insufficiently explored, particularly in the context of nanomaterial-based therapeutic systems. While significant progress has been made in understanding basic metabolic pathways, the dynamic interactions between engineered nanomaterials and biological systems are still not fully elucidated. This knowledge gap is especially evident in the area of in vivo biosafety validation, where existing data often lack the depth and breadth required for comprehensive risk assessment. To address these challenges, it is essential to develop systematic theoretical and statistical models capable of evaluating a wide range of physiological parameters. These include, but are not limited to, biodistribution patterns across different organ systems, metabolic fate and clearance mechanisms, long-term biological effects, potential biotoxicity at both cellular and systemic levels, and detailed immunogenicity profiles. Such models would enable researchers to generate predictive frameworks for assessing the safety and efficacy of nanotherapeutic agents under diverse physiological and pathological conditions.

Although cascaded nanozymes offer advantages such as high catalytic efficiency and robust environmental adaptability in biomedical applications, several challenges remain to be addressed. These include the elucidation of catalytic mechanisms, regulation of enzyme activity, substrate selectivity, and the scalability of large-scale production. To advance this field, three strategic directions are proposed: 1) Atomic-scale biocatalytic engineering: Precise structural and dimensional control of cascade enzymes at the atomic level facilitates the investigation of structure-activity relationships and enhances catalytic performance. Integrated single-atom catalysis enables electron density redistribution, accelerates catalytic turnover, and preserves ROS/pH-responsive behavior through synergistic modulation. 2) Precision molecular recognition design: Current nanozymes primarily mimic the general catalytic functions of natural enzymes but often lack disease-specific targeting capabilities. Advanced architectures incorporating protein-mimetic binding pockets or molecularly imprinted matrices can enable target-specific recognition via multivalent interactions, thereby improving lesion-specific catalytic precision. 3) Integrated catalytic system engineering: The precise regulation of multi-enzyme cascade activities necessitates computational prediction of enzymatic performance. By combining molecular dynamics simulations with artificial intelligence, optimal catalytic parameters can be determined. However, most current studies emphasize therapeutic outcomes rather than mechanistic understanding. Therefore, deeper investigations into cascade reaction mechanisms are essential to establish systematic principles and facilitate clinical translation. At present, most nanozymes are still at the stage of preliminarily verifying therapeutic effects. In the future, more in-depth studies in biocompatibility research, toxicity research and pharmacokinetic research are needed. Future developments should focus on addressing these issues, refining delivery

mechanisms, and exploring combination therapies to maximize their therapeutic potential against inflammatory diseases. By bridging catalytic nanotechnology with systems immunology, cascade nanozymes are poised to redefine precision medicine, offering a transformative framework that simultaneously addresses oxidative stress, cytokine dysregulation, and tissue regeneration–a tripartite therapeutic axis previously unattainable through conventional approaches. Their clinical translation, though challenging, promises to unlock unprecedented therapeutic windows for inflammatory pathologies.

Declaration of competing interest

The authors declare that they have no known competing financial interests or personal relationships that could have appeared to influence the work reported in this paper.

Acknowledgments

The work is supported by the National Key Research and Development Program of China (2022YFC2304700), the Natural Science Foundation of Shanghai (25ZR1403006), the Fundamental Research Funds for the Central Universities (YG2023QNA04).

Data availability

No data was used for the research described in the article.

References

[1] T. Fulop, A. Larbi, G. Pawelec, A. Khalil, A.A. Cohen, K. Hirokawa, J. M. Witkowski, C. Franceschi, Clin. Rev. Allergy Immunol. 64 (2021) 109–122.
[2] A. Chen, H. Huang, S. Fang, Q. Hang, BBA-Rev. Cancer 1879 (2024) 189175.
[3] Y. Qi, B. Rajbanshi, R. Hao, Y. Dang, C. Xu, W. Lu, L. Dai, B. Zhang, X. Zhang, Exp. Mol. Med. 57 (2025) 298–311.
[4] M. Levi, Cardiovasc. Res. 60 (2003) 26–39.
[5] K. Honda, D.R. Littman, Annu. Rev. Immunol. 30 (2012) 759–795.
[6] G.M. Barton, J. Clin. Invest. 118 (2008) 413–420.
[7] O. Takeuchi, S. Akira, Cell 140 (2010) 805–820.
[8] S.L. Carroll, C. Pasare, G.M. Barton, Immunity 57 (2024) 632–648.
[9] R. Chen, J. Zou, J. Chen, X. Zhong, R. Kang, D. Tang, Signal Transduct. Target. Ther. 10 (2025) 216.
[10] H. Su, X. Wang, L. Wang, N. Yuan, Cell Biochem. Biophys. 83 (2024) 73–86.
[11] S.U. Shabana, U. Shahid, S. Irfan, S. Hayat, Sarwar, Acta Diabetol. 62 (2025) 1183–1194.
[12] Y.-S. Lin, Y.-C. Chang, T.-Y. Pu, T.-H. Chuang, L.-C. Hsu, J. Biomed. Sci. 32 (2025) 56.
[13] X. Xu, X. Wu, G. Yue, Q. An, J. Lou, X. Yang, Z. Jin, J. Ding, Y. Hu, Q. Du, J. Xu, R. Xie, Mol. Cell. Biochem. 478 (2022) 1397–1410.
[14] J. Jin, T.-J. Zhou, G.-L. Ren, L. Cai, X.-M. Meng, Acta Pharmacol. Sin. 43 (2022) 2789–2806.
[15] J.E. Stok, M.E. Vega Quiroz, A.G. van der Veen, J. Immunol. 205 (2020) 883–891.
[16] Q. Guo, Y. Jin, X. Chen, X. Ye, X. Shen, M. Lin, C. Zeng, T. Zhou, J. Zhang, Signal Transduct. Target. Ther. 9 (2024) 53.
[17] H. Yu, L. Lin, Z. Zhang, H. Zhang, H. Hu, Signal Transduct. Target. Ther. 5 (2020) 209.
[18] H. Mao, X. Zhao, S.-C. Sun, Cell. Mol. Immunol. 22 (2025) 811–839.
[19] A. Alaimo, S. Genovesi, N. Annesi, D. De Felice, S. Subedi, A. Macchia, F. La Manna, Y. Ciani, F. Vannuccini, V. Mugoni, M. Notarangelo, M. Libergoli, F. Broso, R. Taulli, U. Ala, A. Savino, M. Cortese, S. Mirzaaghaei, V. Poli, I. M. Bonapace, M.G. Papotti, L. Molinaro, C. Doglioni, O. Caffo, A. Anesi, M. Nagler, G. Bertalot, F.G. Carbone, M. Barbareschi, U. Basso, E. Dassi, M. Pizzato, A. Romanel, F. Demichelis, M. Kruithof-de Julio, A. Lunardi, EMBO J. 43 (2024) 780–805.
[20] G.Y. Chen, G. Nuñez, Nat. Rev. Immunol. 10 (2010) 826–837.
[21] Y. Huang, W. Jiang, R. Zhou, Nat. Rev. Immunol. 24 (2024) 703–719.
[22] K. Tanaka, M. Heil, Annu. Rev. Phytopathol. 59 (2021) 53–75.
[23] G. Srikrishna, H.H. Freeze, Neoplasia 11 (2009) 615–628.
[24] S. Paik, J.K. Kim, H.J. Shin, E.-J. Park, I.S. Kim, E.-K. Jo, Cell. Mol. Immunol. 22 (2025) 563–596.
[25] R. Ramachandran, A. Manan, J. Kim, S. Choi, Exp. Mol. Med. 56 (2024) 1488–1500.
[26] L. Vande Walle, M. Lamkanfi, Nat. Rev. Drug Discov. 23 (2023) 43–66.
[27] W. Xu, Y. Huang, R. Zhou, Cell. Mol. Immunol. 22 (2025) 341–355.
[28] K.V. Swanson, M. Deng, J.P.Y. Ting, Nat. Rev. Immunol. 19 (2019) 477–489.
[29] P.D. Ray, B.-W. Huang, Y. Tsuji, Cell. Signal. 24 (2012) 981–990.
[30] G. Di Dalmazi, J. Hirshberg, D. Lyle, J.B. Freij, P. Caturegli, Autoimmun. Highlights 7 (2016) 11.
[31] B.C. Dickinson, C.J. Chang, Nat. Chem. Biol. 7 (2011) 504–511.
[32] G. Pizzino, N. Irrera, M. Cucinotta, G. Pallio, F. Mannino, V. Arcoraci, F. Squadrito, D. Altavilla, A. Bitto, Oxidative Med. Cell. Longev. (2017 (2017) 8416763.
[33] C. Murdoch, M. Zhang, A. Cave, A. Shah, Cardiovasc. Res. 71 (2006) 208–215.
[34] W. Liu, H. Wu, L. Chen, Y. Wen, X. Kong, W.-Q. Gao, Cell Res. 25 (2015) 691–706.
[35] F.-X. Lin, H.-Y. Gu, W. He, Exp. Neurol. 383 (2025) 115043.
[36] A. Shi, L. Liu, S. Li, B. Qi, J. Cancer Res. Clin. Oncol. 150 (2024) 6.
[37] B. Halliwell, Nat. Rev. Mol. Cell Biol. 25 (2023) 13–33.
[38] B. Hu, Y. Ouyang, T. Zhao, Z. Wang, Q. Yan, Q. Qian, W. Wang, S. Wang, Adv. Healthc. Mater. 13 (2024) 2303817.
[39] Y. Zhu, K. Wang, X. Jia, C. Fu, H. Yu, Y. Wang, Med. Res. Rev. 44 (2023) 275–364.
[40] Y. Chen, B. Li, K. Li, Y. Lin, Chem. Commun. 60 (2024) 4140–4147.
[41] S. König, F. Strassheimer, N.I. Brandner, J.-H. Schröder, H. Urban, L.F. Harwart, S. Hehlgans, J.P. Steinbach, M.W. Ronellenfitsch, A.-L. Luger, Cell Death Dis. 10 (2024) 379..
[42] G. Schanne, S. Demignot, C. Policar, N. Delsuc, Coord. Chem. Rev. 514 (2024) 215906.
[43] C. Glorieux, P. Buc Calderon, Redox Biol. 77 (2024) 103404.
[44] R.S. Riseh, F. Fathi, M. Vatankhah, J.F. Kennedy, Int. J. Biol. Macromol. 280 (2024) 135859.
[45] S. He, M. Lin, Q. Zheng, B. Liang, X. He, Y. Zhang, Q. Xu, H. Deng, K. Fan, W. Chen, Adv. Healthc. Mater. 13 (2024) 2303548.
[46] Y. Liao, Z. Zhang, Y. Zhao, S. Zhang, K. Zha, L. Ouyang, W. Hu, W. Zhou, Y. Sun, G. Liu, Bioactive Mater. 44 (2025) 131–151.
[47] P. Amadio, L. Sandrini, M. Zarà, S.S. Barbieri, A. Ieraci, Redox Biol. 70 (2024) 103060.
[48] X. Zhang, D. Zhang, C. Zhong, W. Li, S.P. Dinesh-Kumar, Y. Zhang, New Phytol. 245 (2024) 510–522.
[49] D. Kračun, L.R. Lopes, E. Cifuentes-Pagano, P.J. Pagano, Physiol. Rev. 105 (2025) 1291–1428.
[50] W. Lai, W. Zhu, J. Wu, J. Huang, X. Li, Y. Luo, Y. Wang, H. Zeng, M. Li, X. Qiu, X. Wen, Redox Biol. 77 (2024) 103392.
[51] G. Antonio, S. Minero, A. Møllebjerg, C. Thiesen, Mikkel I. Johansen, Nis P. Jørgensen, V. Birkedal, D.E. Otzen, Rikke L. Meyer, Nucleic Acids Res. 52 (2024) 1575–1590.
[52] L. Flohé, S. Toppo, L. Orian, Free Radic. Biol. Med. 187 (2022) 113–122.
[53] M. Ma, W. Jiang, R. Zhou, Immunity 57 (2024) 752–771.
[54] M.P. Murphy, L.A.J. O'Neill, Nature 626 (2024) 271–279.
[55] E. Ricca, B. Brucher, J.H. Schrittwieser, Adv. Synth. Catal. 353 (2011) 2239–2262.
[56] J. Sheng, Y. Wu, H. Ding, K. Feng, Y. Shen, Y. Zhang, N. Gu, Adv. Mater. 36 (2023) 2211210.
[57] X. Cai, Y. Huang, C. Zhu, Adv. Healthc. Mater. 14 (2025) 2401834.
[58] X. Meng, H. Fan, L. Chen, J. He, C. Hong, J. Xie, Y. Hou, K. Wang, X. Gao, L. Gao, X. Yan, K. Fan, Nat. Commun. 15 (2024) 1626.
[59] D. Li, D. Dai, G. Xiong, S. Lan, C. Zhang, Small 19 (2023) 2205870.
[60] X. Liu, Y. Yang, X. Wang, X. Liu, H. Cheng, P. Wang, Y. Shen, A. Xie, M. Zhu, J. Mater. Chem. B 9 (2021) 6396–6405.
[61] F. Nan, Q. Jia, X. Xue, S. Wang, W. Liu, J. Wang, J. Ge, P. Wang, Biomaterials 284 (2022) 121495.
[62] N. Singh, M.A. Savanur, S. Srivastava, P. D'Silva, G. Mugesh, Angew. Chem. Int. Ed. 56 (2017) 14267–14271.
[63] S. Liu, L. Fang, H. Ding, Y. Zhang, W. Li, B. Liu, S. Dong, B. Tian, L. Feng, P. Yang, ACS Nano 16 (2022) 20805–20819.
[64] A.I. Benítez-Mateos, D. Roura Padrosa, F. Paradisi, Nat. Chem. 14 (2022) 489–499.
[65] Y.-P. Xiao, J. Wu, P.-H. Chen, S. Lei, J. Lin, X. Zhou, P. Huang, Chem. Soc. Rev. 54 (2025) 3247–3271.
[66] X. Cai, L. Jiao, H. Yan, Y. Wu, W. Gu, D. Du, Y. Lin, C. Zhu, Mater. Today 44 (2021) 211–228.
[67] W.R. Birmingham, N.J. Turner, ACS Catal. 8 (2018) 4025–4032.
[68] G. Li, X. Guo, J. Luo, J. Guo, S. Xiao, X. Yang, X. Shi, J. Xiang, J. Yang, T. Ma, C. Lu, L. Zheng, J. Zhao, J. Zhong, Nano Today 56 (2024) 102250.
[69] S. Zhang, Y. Zhang, Y. Feng, J. Wu, Y. Hu, L. Lin, C. Xu, J. Chen, Z. Tang, H. Tian, X. Chen, Adv. Mater. 34 (2022) 2206851.
[70] L. Zhou, K. Lan, X. Huang, Y. Huang, Y. Jin, S. Lu, Y. Guo, L. Su, Y. Peng, Z. Deng, J. Yang, S. Qian, W. Lou, X. Chu, H. Guo, B. Wang, Adv. Funct. Mater. 33 (2023) 2302493.
[71] C. Cao, H. Zou, N. Yang, H. Li, Y. Cai, X. Song, J. Shao, P. Chen, X. Mou, W. Wang, X. Dong, Adv. Mater. 33 (2021) 2106996.
[72] H. Liu, Z. Wang, X. Hu, S. Rao, H. Wang, H. Xie, Adv. Healthc. Mater. 14 (2025) 2501111.
[73] M. Lubberink, C. Schnepel, J. Citoler, S.R. Derrington, W. Finnigan, M.A. Hayes, N.J. Turner, S.L. Flitsch, ACS Catal. 10 (2020) 10005–10009.
[74] D. Roura Padrosa, A.I. Benítez-Mateos, L. Calvey, F. Paradisi, Green Chem. 22 (2020) 5310–5316.
[75] Z. Zhou, X. Mei, K. Hu, M. Ma, Y. Zhang, ACS Appl. Mater. Interfaces 15 (2023) 17612–17626.
[76] B.R. Lichman, E.D. Lamming, T. Pesnot, J.M. Smith, H.C. Hailes, J.M. Ward, Green Chem. 17 (2015) 852–855.
[77] M. Li, J. Liu, L. Shi, C. Zhou, M. Zou, D. Fu, Y. Yuan, C. Yao, L. Zhang, S. Qin, M. Liu, Q. Cheng, Z. Wang, L. Wang, Bioactive Mater. 25 (2023) 95–106.
[78] J. Cheng, Y. Zhang, L. Ma, W. Du, Q. Zhang, R. Gao, X. Zhao, Y. Chen, L. Jiang, X. Li, B. Li, Y. Zhou, Adv. Sci. 10 (2023) 2304002.

[79] J. Guo, C. Li, J. Lin, J. Fang, Y. Sun, P. Zhang, S. Li, W. Li, X. Zhang, Chem. Eng. J. 485 (2024) 149897.
[80] K. Xiang, H. Wu, Y. Liu, S. Wang, X. Li, B. Yang, Y. Zhang, L. Ma, G. Lu, L. He, Q. Ni, L. Zhang, Theranostics 13 (2023) 2721–2733.
[81] Z. Wang, Y. Zhao, Y. Hou, G. Tang, R. Zhang, Y. Yang, X. Yan, K. Fan, Adv. Mater. 36 (2023) 2210144.
[82] T. Xiong, K. Yang, T. Zhao, H. Zhao, X. Gao, Z. You, C. Fan, X. Kang, W. Yang, Y. Zhuang, Y. Chen, J. Dai, Adv. Sci. 10 (2023) 2205997.
[83] H. He, Q. Zhang, Y. Zhang, S. Qu, B. Li, J. Lin, X. Lu, C. Xie, Nat. Commun. 16 (2025) 2768.
[84] F. Gao, W. Liang, Q. Chen, B. Chen, Y. Liu, Z. Liu, X. Xu, R. Zhu, L. Cheng, Nanomaterials 14 (2024) 389.
[85] W. Wang, J. Duan, W. Ma, B. Xia, F. Liu, Y. Kong, B. Li, H. Zhao, L. Wang, K. Li, Y. Li, X. Lu, Z. Feng, Y. Sang, G. Li, H. Xue, J. Qiu, H. Liu, Adv. Sci. 10 (2023) 2205859.
[86] J. Mu, C. Li, Y. Shi, G. Liu, J. Zou, D.-Y. Zhang, C. Jiang, X. Wang, L. He, P. Huang, Y. Yin, X. Chen, Nat. Commun. 13 (2022) 2513.
[87] Q. Wang, C. Cheng, S. Zhao, Q. Liu, Y. Zhang, W. Liu, X. Zhao, H. Zhang, J. Pu, S. Zhang, H. Zhang, Y. Du, H. Wei, Angew. Chem. Int. Ed. 61 (2022) e202201101.
[88] H. Yuan, F. Wang, Z. Wang, D. Gu, W. Huang, C. Fu, X. Wang, J. Ma, Z. Li, L. Dai, X. Zhang, W. Xiao, J. Wang, ACS Mater. Lett. 5 (2023) 2807–2819.
[89] X. Du, B. Jia, W. Wang, C. Zhang, X. Liu, Y. Qu, M. Zhao, W. Li, Y. Yang, Y.-Q. Li, J. Nanobiotechnol. 20 (2022) 12.
[90] M. Wu, L. Lu, J. Li, Q. Guo, D. Wang, Y. Gong, X. Wu, X. Zhao, X. Zhang, Y. Zhao, X. Li, Adv. Funct. Mater. 33 (2023) 2301664.
[91] X. Zhang, S. Zhang, Z. Yang, Z. Wang, X. Tian, R. Zhou, Nanoscale 13 (2021) 12613–12622.
[92] L. Shang, Y. Yu, Y. Jiang, X. Liu, N. Sui, D. Yang, Z. Zhu, ACS Nano 17 (2023) 15962–15977.
[93] L.-H. Fu, M. Yin, X. Chen, C. Yang, J. Lin, X. Wang, B. Jiang, P. Huang, Nano Lett. 25 (2025) 3075–3084.
[94] R. Tian, H. Ma, W. Ye, Y. Li, S. Wang, Z. Zhang, S. Liu, M. Zang, J. Hou, J. Xu, Q. Luo, H. Sun, F. Bai, Y. Yang, J. Liu, Adv. Funct. Mater. 32 (2022) 2204025.
[95] S. Honap, V. Jairath, S. Danese, L. Peyrin-Biroulet, Nat. Rev. Drug Discov. 23 (2024) 546–562.
[96] I.D. Iliev, A.N. Ananthakrishnan, C.-J. Guo, Nat. Rev. Microbiol. 23 (2025) 509–524.
[97] S. Vieujean, V. Jairath, L. Peyrin-Biroulet, M. Dubinsky, M. Iacucci, F. Magro, S. Danese, Nat. Rev. Gastroenterol. Hepatol. 22 (2025) 371–394.
[98] Y. Chen, J. Feng, Y. Chen, C. Xia, M. Yao, W. Ding, X. Li, X. Fu, S. Zheng, Y. Ma, J. Zou, M. Lan, F. Gao, Int. J. Pharm. 659 (2024) 124117.
[99] Y. Yu, D. Yang, B. Lin, L. Zhu, C. Li, X. Li, ACS Nano 18 (2024) 13583–13598.
[100] K. Kwon, J. Jung, A. Sahu, G. Tae, J. Control. Release 344 (2022) 160–172.
[101] Q.-W. Chen, M.-W. Cao, J.-Y. Qiao, Q.-R. Li, X.-Z. Zhang, Nanoscale Horizons 8 (2023) 489–498.
[102] Y. Liu, Y. Cheng, H. Zhang, M. Zhou, Y. Yu, S. Lin, B. Jiang, X. Zhao, L. Miao, C. W. Wei, Q. Liu, Y.W. Lin, Y. Du, C.J. Butch, H. Wei, Sci. Adv. 6 (2020) eabb2695.
[103] Y. Yu, X. Zhao, X. Xu, C. Cai, X. Tang, Q. Zhang, L. Zhong, F. Zhou, D. Yang, Z. Zhu, Adv. Mater. 35 (2023) 2304967.
[104] F. Muhammad, X. Chen, J. Tang, Y. Cheng, Y. Li, C. Zhu, Y. Zhang, L. Miao, Y. Deng, H. Wei, Chem. Sci. 15 (2024) 1679–1691.
[105] Z. Han, K. Wang, S. Ding, M. Zhang, Bone Res. 12 (2024) 69.
[106] M.H.J. van den Bosch, A.B. Blom, P.M. van der Kraan, Osteoarthr. Cartil. 32 (2024) 355–364.
[107] Y. Fan, Z. Niu, L. Yin, L. Yao, S. Ding, Y. Tong, J. Wang, Z. Hong, J. Chen, Q. Zhang, L. Ji, J. Chen, C. Xia, Q. Bi, Mater. Today Bio 32 (2025) 101778.
[108] J. Xu, Y. Yu, K. Chen, Y. Wang, Y. Zhu, X. Zou, X. Xu, Y. Jiang, Int. J. Biol. Macromol. 258 (2024) 129004.
[109] B. Yu, W. Sun, J. Lin, C. Fan, C. Wang, Z. Zhang, Y. Wang, Y. Tang, Y. Lin, D. Zhou, Advanced Science 11 (2024) 2307798.
[110] Y. Gong, J. Huang, X. Xing, H. Liu, Z. Zhou, H. Dong, Chem. Eng. J. 481 (2024) 148523.
[111] Q. Geng, J. Xu, X. Cao, Z. Wang, Y. Jiao, W. Diao, X. Wang, Z. Wang, M. Zhang, L. Zhao, L. Yang, T. Deng, B. Fan, Y. Xu, L. Jia, C. Xiao, J. Autoimmun. 146 (2024) 103214.
[112] C.S. Martin, A. Crastin, M.S. Sagmeister, M.S. Kalirai, J.D. Turner, L. MacDonald, M. Kurowska-Stolarska, D. Scheel-Toellner, A.E. Taylor, L.C. Gilligan, K. Storbeck, M. Price, C.M. Gorvin, Filer A, R. Mahida, A.R. Clark, S.W. Jones, K. Raza, M. Hewison, R.S. Hardy, J. Autoimmun. 147 (2024) 103263.
[113] Z. Tang, S. Meng, X. Yang, Y. Xiao, W. Wang, Y. Liu, K. Wu, X. Zhang, H. Guo, Y. Z. Zhu, X. Wang, Small 20 (2024) 2307379.
[114] Q. Xu, Y. Ma, R. Dai, L. Wang, J. Li, Q. Liu, L. Chen, S. Wu, L. Xin, Z. Zheng, J. Gao, Mater. Des. 257 (2025) 114389.
[115] M. Jia, W. Ren, Y. Liu, C. Wang, X. Zheng, D. Zhang, X. Tan, C. Li, ACS Appl. Mater. Interfaces 15 (2022) 338–353.
[116] Y. Wang, J. Wang, S.Y. Tao, Z. Liang, R. Xie, N.N. Liu, R. Deng, Y. Zhang, D. Deng, G. Jiang, Diabetes Metab. Res. Rev. 40 (2024) e3733.
[117] M. Martiniakova, R. Biro, V. Kovacova, M. Babikova, N. Zemanova, V. Mondockova, R. Omelka, J. Mol. Med. 102 (2024) 435–452.
[118] M. Chang, T.T. Nguyen, Acc. Chem. Res. 54 (2021) 1080–1093.
[119] Y. Yuan, Y. Yang, Z. Ji, J. Feng, L. Shu, S. Xiao, Z. Huang, Chem. Eng. J. 505 (2025) 159537.
[120] Z. Cai, L. Bai, Q. Li, Y. Li, X. Cai, Y. Lin, ACS Nano 18 (2024) 35214–35229.
[121] J.Q. Li, B. Li, Z.Q. Fei, S.S. Lei, FASEB J. 38 (2024) e70074.
[122] C. Li, H. Gong, P. Shi, S. Liu, Q. Zhang, Int. J. Mol. Sci. 26 (9) (2025) 4417.
[123] H. Fang, M. Xu, J. Zhang, H. Qin, H. Tang, Y. He, W. Guo, BBA-Mol. Basis Dis. 1870 (2024) 167496.
[124] W. Zhang, J. Liu, P. Li, X. Wang, B. Tang, Acc. Chem. Res. 57 (2024) 2594–2605.
[125] Y. Jin, J. Zhang, Y. Xu, K. Yi, F. Li, H. Zhou, H. Wang, H.F. Chan, Y.-H. Lao, S. Lv, Y. Tao, M. Li, Bioactive Mater. 28 (2023) 112–131.
[126] J. Zhang, T. Zhang, Z. Zhang, Q. Jia, J. Chen, J. Li, H. Song, J. Li, Y. Xiong, L. Mo, J. He, Y. Li, Adv. Funct. Mater. 34 (2024) 2404658.
[127] X. Ding, X.-L. Zhu, D.-H. Xu, S. Li, Q. Yang, X. Feng, Y.-G. Wei, H. Li, L. Yang, Y.-J. Zhang, X.-L. Deng, K.-C. Liu, S.-L. Shi, Cell Death Dis. 14 (2023) 575.
[128] D. Zhang, Y.-H. Zhang, B. Liu, H.-X. Yang, G.-T. Li, H.-L. Zhou, Y.-S. Wang, Metabolism 166 (2025) 156173.
[129] Y. Feng, X. Zhang, J. Li, S. Fu, W. Xu, J. Liu, Y. Yang, T. Chen, Y. Zhao, D. Li, M. Zhang, Y. He, Theranostics 15 (2025) 1035–1056.
[130] F. Wang, H. Yuan, J. Shen, Z. Li, J. Li, P. Luo, Q. Zhang, W. Huang, X. Wang, J. Ma, W. Zhang, C. Fu, J. Sun, X. Sun, J. Wang, W. Xiao, ACS Mater. Lett. 6 (2024) 1304–1316.
[131] X. Ba, T. Ye, H. Shang, Y. Tong, Q. Huang, Y. He, J. Wu, W. Deng, Z. Zhong, X. Yang, K. Wang, Y. Xie, Y. Zhang, X. Guo, K. Tang, ACS Appl. Mater. Interfaces 16 (2024) 12117–12148.
[132] J.-H. Wang, H.-B. Mao, J.-B. Hu, S. Cheng, H. Su, J. Control. Release 376 (2024) 1100–1114.
[133] C. Huang, Y. Deng, R. Ma, H. Ge, F. Gong, J. Yang, X. Zhu, Y. Wang, Nanoscale 16 (2024) 9406–9411.
[134] A. Sahu, K. Min, S.H. Jeon, K. Kwon, G. Tae, Carbohydr. Polym. 316 (2023) 121088.
[135] N. Hu, M. Sun, N. Lv, Y. Gao, X. Fu, D. Xing, X. Guo, S. Zhai, R. Zhang, ACS Appl. Mater. Interfaces 16 (2024) 12188–12201.
[136] M. Sun, N. Hu, Y. Gao, N. Lv, X. Fu, Y. Li, S. Zhai, R. Zhang, Adv. Healthc. Mater. 13 (2024) 2303101.
[137] Z. Dong, L. Tang, Y. Zhang, X. Ma, Y. Yin, L. Kuang, Q. Fan, B. Wang, X. Hu, T. Yin, Y. Wang, Adv. Funct. Mater. 34 (2024) 2309167.
[138] M. Sun, J. Ma, G. Zhang, M. Song, R. Lv, J. Liang, Y. Shi, L. Zhao, ACS Nano 19 (2025) 15491–15508.
[139] Y. Yang, Z. Li, X. Fan, C. Jiang, J. Wang, Y. Rastegar-Kashkooli, T.J. Wang, J. Wang, M. Wang, N. Cheng, X. Yuan, X. Chen, B. Jiang, J. Wang, ACS Nano 18 (2024) 16450–16467.
[140] C. Jian, Y. Hong, H. Liu, Q. Yang, S. Zhao, Int. J. Pharm. 669 (2025) 125087.
[141] A. Xie, G. Cheng, J. Wu, Z. Li, G. Yu, X. Zhu, T. Chen, Biomaterials 312 (2025) 122749.
[142] B. Kalyanaraman, G. Cheng, M. Hardy, Redox Biol. 71 (2024) 103092.
[143] Z. Liu, C. Xiang, X. Zhao, T. Aizawa, R. Niu, J. Zhao, F. Guo, Y. Li, W. Luo, W. Liu, R. Gu, J. Nanobiotechnol. 22 (2024) 767.
[144] J. Liu, T. Wang, C. Liao, W. Geng, J. Yang, S. Ma, W. Tian, L. Liao, C. Cheng, Adv. Mater. 36 (2024) 2411618.
[145] Z. Yin, B. Wan, G. Gong, J. Yin, Front. Immunol. 15 (2024) 1330678.
[146] Q. Tian, S. Li, Z. Tang, Z. Zhang, D. Du, X. Zhang, X. Niu, Y. Lin, Adv. Healthc. Mater. 14 (2025) 2401630.
[147] N. Tagaras, H. Song, S. Sahar, W. Tong, Z. Mao, T. Buerki-Thurnherr, Advanced Science 11 (2024) 2407816.
[148] M. Ghorbani, H. Derakhshankhah, S. Jafari, S. Salatin, M. Dehghanian, M. Falahati, A. Ansari, Nano Today 29 (2019) 100775.
[149] Y. Wang, X. Jia, S. An, W. Yin, J. Huang, X. Jiang, Adv. Mater. 36 (2024) 2301810.